fied Eagle's medium (DMEM; Nissui) supplemented with 10% FCS. U87MG was maintained in DMEM supplemented with 20% FCS. HUK-1, NP2 and U251 were maintained in Eagle's medium (Nissui) supplemented with 10% FCS. The maintenance of PH5CH8 cells was previously described in detail [23]. Human brain microvascular endothelial cells (HBMECs, Applied Cell Biology Research Institute, WA) were maintained in endothelial cell basal medium 2 supplemented with EGM-2 additives (Clontecs, CA). Human brain pericytes (HBP) were derived from surgically dissected human brain tissue. HBP cells were maintained in RPMI-1640 medium supplemented with 10% FCS, 10 μg/ml of endothelial cell growth supplement, and 10 ng/ml of epidermal growth factor. All culture media were supplemented with 50 μg/ml of kanamycin before use.

2.2. Plasmids

Fragments of the HCV C, E1 and E2 genes were obtained from a subclone of an infectious clone of HCV, subtype Ib [6], the predominant subtype in Japan, and cloned into pCXbsr, a Moloney murine leukemia virus-based retroviral vector plasmid [24]. Mammalian expression plasmids encoding HCV core protein (pCXbsr/C), HCV E1 protein (pCXbsr/E1), HCV E2 protein (pCXbsr/E2) and all HCV structural proteins, core-E1–E2 (pCXbsr/CE1E2), were made as shown in Fig. 1b. To construct retroviral expression plasmids encoding chimeric HCV envelope proteins, we generated the plasmid pCAGGS/TM, encoding the signal sequence, the transmembrane domain, and the cytoplasmic tail of the VSV G protein, as described below. pCAGGS/TM was amplified by PCR using pCAGGS/VSV-G [25] as a template, in which VSV (Indiana serotype) G protein was placed under control of the CAG promoter, and the following primers:

- sense primer, 5′-AAAAGCTCTATTGCCTCTTTTT-TCTTTATC;
- antisense primer, 5′-GCAATTCACCCCAATGAATA-AAAAGGCTAA.

The coding sequence for the ectodomain of HCV E1 (aa 192–340) was amplified by PCR using pCXbsr/CE1E2 as a template and the following primers:

- sense primer, 5′-TATGAAGTGCGCAACGTGTCCGG-GGTGTAC;
- antisense primer, 5′-GATCCGGAGCAACTGCGA-TACCACCAGGGC.

The ectodomain of the HCV E2 (aa 384–715) genomic region was amplified by PCR using pCXbsr/CE1E2 as a template and the following primers:

- sense primer, 5′-GCTACCTACACGTCAGGGGGGAC-GGTAGGC;
- antisense primer, 5′-TCTGATTACAACGGAGACAAC-CACTGACCC.

The ectodomains of E1 and E2 sequences were subcloned into pCAGGS/TM, using a Blunting High kit (Toyobo, Tokyo, Japan), and the plasmids pCAGGS/E1TM and pCAGGS/E2TM were isolated. pCAGGS/E1TM and pCAGGS/E2TM digested with *Eco*RI (Takara, Siga, Japan) were subcloned into pCXbsr, resulting in the formation of pCXbsr/E1TM and pCXbsr/E2TM, respectively (Fig. 1b).

2.3. Immunofluorescence staining of E1 and E2

293T cells were seeded onto slide glasses and the next day transfected with the expression plasmid vectors for HCV envelope proteins using FuGENE6 (Roche, Basel, Switzerland). After 32 h, the cells were tested for the expression of the viral envelope proteins by indirect immunofluorescence. Namely, the cells were washed with phosphate-buffered saline (PBS) and fixed with 4% paraformaldehyde in PBS for 5 min at room temperature. Half the fixed cell samples were then permeabilized with 0.1% Triton X-100 for 5 min at room temperature. A mouse monoclonal antibody (MAb) to E1, E1-384 [26], and a rat MAb to E2, Mo-12 [27], were used as follows. The MAb diluted to 1:1000 in PBS was added as the primary antibody and incubated for 60 min at 37 °C. After a wash with PBS, fluorescein isothiocyanate (FITC)-conjugated rat anti-mouse IgG or FITC-conjugated rabbit anti-rat IgG (Dako, Glostrup, Denmark) diluted 1:50 in PBS was added, and the cells were incubated for 60 min at 37 °C. After three washes in PBS, the cells seeded on slide glasses were embedded with a solution of glycerol in PBS and examined with a fluorescence microscope for the expression of HCV glycoproteins.

2.4. Preparation of pseudotype viruses

VSVΔG*G is the recombinant VSV, generated by reverse genetics, as described previously [18] and kindly provided by Dr. M.A. Whitt. To generate VSV pseudotype viruses, 2×10^6 293T cells were grown in a poly-L-lysine-coated 60-mm dish and transfected with plasmids. Thirty-two hours after transfection, the cells were infected with VSVΔG*G at an MOI of 2 for 2.5 h at 37 °C in a 5% CO_2 incubator. Virus-infected cells were washed with serum-free DMEM and incubated in 1 ml of goat anti-VSV polyclonal antibody (diluted at 1:10) for 40 min at 37 °C to neutralize unabsorbed virus. This concentration was enough to completely neutralize the undiluted VSVΔG*G. Then, they were again washed with serum-free DMEM four times, and culture medium was added. After 15 h of incubation at 37 °C, the culture supernatants + adherent cells were harvested and centrifuged at 350 × *g* for 3 min at room temperature. Then, cell pellets were either sonicated or left untreated, and the virus samples were clarified by centrifugation at 350 × *g* for 5 min at room temperature to remove cell debris. Virus samples were stock frozen at –80 °C. These samples were found to show compatible properties with those of HCV virions, as described in Table 2. As control pseudotypes, VSVΔG*G and VSVΔG* were used. VSVΔG*G was prepared by infecting 293T cells that had been transfected with pCAGGS/VSV-G, while the VSVΔG* sample was prepared by infecting 293T cells that had been transfected with pCXbsr plasmid containing no envelope protein.

2.5. Detection of HCV envelope proteins and VSV structural proteins in pseudotype virus samples by Western blotting

We prepared 293T cells transfected with the expression plasmid vectors for HCV envelope proteins described in Table 2. These cells were infected with VSVΔG*G. We also prepared the 293T cells transfected with the expression plasmid vectors for HCV envelopes that were not infected with VSVΔG*G. These samples were sonicated and centrifuged at 350 × *g* for 5 min. Each 3-ml supernatant was subjected to ultracentrifugation (27,000 rpm for 3 h at 4 °C) through 2 ml of a 20% sucrose layer using an SCP70H HITACHI. Pellets were suspended in 30 μl of sample buffer (1% SDS, 1% 2-mercaptomethanol, 50 mM Tris–HCl [pH 6.8], and 20% glycerol). The samples were loaded onto 10% SDS-PAGE gel. E1 proteins were detected using an anti-E1 mouse MAb, E1-384 [26] (diluted at 1:1000), and then HRP-conjugated anti-mouse IgG (Dako; diluted at 1:1000). E2 proteins were detected using an anti-E2 rat MAb, Mo-12 [27] (diluted at 1:1000), and HRP-conjugated anti-rat IgG (Dako). VSV structural proteins were detected using goat anti-VSV polyclonal antibody (diluted at 1:4000), and HRP-conjugated anti-goat IgG (Dako). HRP-conjugated antibodies bound to filters were detected using enhanced chemiluminescence.

2.6. Titration of pseudotype viruses using various cell lines

Cells (2×10^4) were seeded into wells of 96-well flat-bottom plates. After 36 h of incubation, the cells were infected with the virus samples defined in Table 2 and incubated at 37 °C for 24 h. The HepG2 cell line was incubated at 33 °C, because a lower temperature had a better effect on infection in this cell line. Infectious units (IU) of the samples were determined by counting the number of GFP-expressing cells under a fluorescence microscope.

2.7. Sonication for preparation of pseudotype virus samples

As the native form of the HCV envelope protein was reported not to be expressed on the cell surface [28,29], we tested a sonication step to efficiently recover HCV pseudotypes. For this, the VSV pseudotype samples harvested as described above were sonicated with a SONIFIER 250 (Branson, CT) for 0.2 s five times on ice. The samples were centrifuged at 350 × *g* for 5 min, and supernatants were aliquoted and stocked frozen at –80 °C. HepG2 cells were used for titration of the pseudotype samples prepared with or without sonication. After 24 h of infection, IU were determined as described above.

2.8. Neutralization of the pseudotype virus samples

To judge whether the infectivity of each virus sample was HCV- or VSV-specific, the pseudotype virus samples were incubated with serially diluted polyclonal antibody against VSV in the presence or absence of human sera from patients with chronic HCV infection (final concentration up to 20%) for 30 min at 37 °C, and HepG2 cells were infected with these samples. After 24 h of incubation, the amount of remaining infectious titer was determined as described above. All previous reports have, however, shown that sera from patients with chronic HCV infection hardly neutralized chimeric E1 or E2 pseudotypes [17,19].

2.9. Treatment of the pseudotype viruses with chemicals

Pseudotype virus samples expected to bear E1, E2 or E1E2 protein were preincubated with various concentrations of bovine lactoferrin (Wako, Tokyo, Japan) at 37 °C for 1 h and inoculated onto HepG2 cells. After 1.5 h of incubation, the cells were washed with DMEM three times and incubated with fresh culture medium. The VSVΔG*(HCV) pseudotype was preincubated with heparin (Wako), dextran sulfate (molecular weight (MW) 8000 or 500,000) or dextran (MW 7000; Sigma, MO) at 37 °C for 1 h, and HepG2 cells in a 96-well plate were infected with these samples. VSVΔG*G was used as a control in most experiments. After 24 h of incubation, each infectious titer was determined as described above.

2.10. Enzymatic and chemical modification of target cells

HepG2 cells in a 96-well plate were washed with PBS and treated with 50 μl of heparitinase (Sigma) for 1 hr, 50 μl of trypsin (Sigma) for 5 min, or 50 μl of α-mannosidase (Sigma) for 1 hr at 37 °C. Subsequently, an equal volume of complete medium was added to stop the enzyme, and then, the cells were washed with PBS and infected with each pseudotype virus sample. HepG2 cells in a 96-well plate were also preincubated in DMEM containing tunicamycin (Sigma) overnight. Then, they were infected with each virus. After 24 h of incubation, the infectious titer was determined.

All the virus titration experiments were done in triplicate. In each figure, the results shown are means, with error bars representing standard deviations (S.D.).

3. Results

3.1. Localization of HCV envelope proteins expressed in 293T cells

We expressed the HCV envelope proteins by transfection with plasmid vectors encoding HCV envelope proteins shown in Table 1. The carboxyl-terminal domains of HCV envelope proteins, E1 and E2, contain ER retention signals [28–30]. To incorporate HCV envelope proteins into VSV particles, it has been reported to be necessary to express these proteins on the cell surface. Thus, to generate HCV pseudotype viruses, chimeric proteins of the ectodomain of HCV E1 or E2, and

Table 1
Detection of HCV envelope proteins by indirect immunofluorescence

Transfected plasmids	Positively stained cells (%)[a]			
	anti-E1		anti-E2	
	(–)[b]	(+)	(–)	(+)
pCXbsr	0	0	0	0
pCXbsr/CE1E2	0	30	0	30
pCXbsr/E1	0	40	0	0
pCXbsr/E2	0	0	0	40
pCXbsr/E1 and pCXbsr/E2	0	40	0	30
pCXbsr/E1, pCXbsr/E2 and pCXbsr/C	0	20	0	30
pCXbsr/E1TM	40	40	0	0
pCXbsr/E2TM	0	0	50	50
pCXbsr/E1TM and pCXbsr/E2TM	30	30	40	40

[a] A mouse monoclonal antibody to E1, E1-384, and a rat monoclonal antibody to E2, Mo-12, were used at a 1/1000 dilution. Percentage of positively stained cells is the mean value from at least three different experiments.

[b] 293T cells were transfected with the indicated plasmid DNA and cultivated for 2 days. The cells were fixed with 4% paraformaldehyde and permeabilized (+), or not (–), with Triton X-100, before immunofluorescence.

the transmembrane domain of VSV G have been used [15–17]. We also made pCXbsr/E1TM and pCXbsr/E2TM encoding the ectodomains of E1 and E2, respectively, joined to the signal sequence, transmembrane and cytoplasmic tail of VSV G protein. In addition, we made plasmid vectors, pCXbsr/CE1E2 coding for the entire HCV structural protein, pCXbsr/C, pCXbsr/E1 and pCXbsr/E2. The structural protein, CE1E2, will be cleaved by cellular signal peptidases [7,8]. Then, we examined the localization of the HCV envelope proteins by indirect immunofluorescence after the fixation of cells with paraformaldehyde (Table 1). Triton X-100-permeabilized cells and non-permeabilized cells were analyzed in parallel. The native forms of the HCV envelope proteins were apparently detected in the transduced cells only after permeabilization. In contrast, the chimeric proteins E1TM and E2TM were observed in both non-permeabilized and permeabilized cells, as reported [16,17].

3.2. Preparation of VSV pseudotypes bearing HCV envelope proteins

3.2.1. Western blotting for HCV envelope proteins

First, to examine whether the native forms of HCV envelope proteins expressed in the cytoplasm in 293T cells could be incorporated into VSV lacking G protein but expressing GFP, VSVΔG* pseudotype virus samples were analyzed by Western blotting (Fig. 2a). E1 was detected as a broad band in a MW range of 30–40 kDa, as previously reported [31,32]. E1 protein in VSVΔG*(HCV) preparation migrated more slowly than E1 protein in VSVΔG*(E1) preparation upon SDS-PAGE. This observation may be explained by different glycosylation of E1 proteins: the glycosylation of E1 has been reported to be enhanced when E1 and E2 are expressed in *cis* [33]. E2 was detected as a discrete band in a MW range of 50–60 kDa, as previously reported [31]. E2 migrated slightly

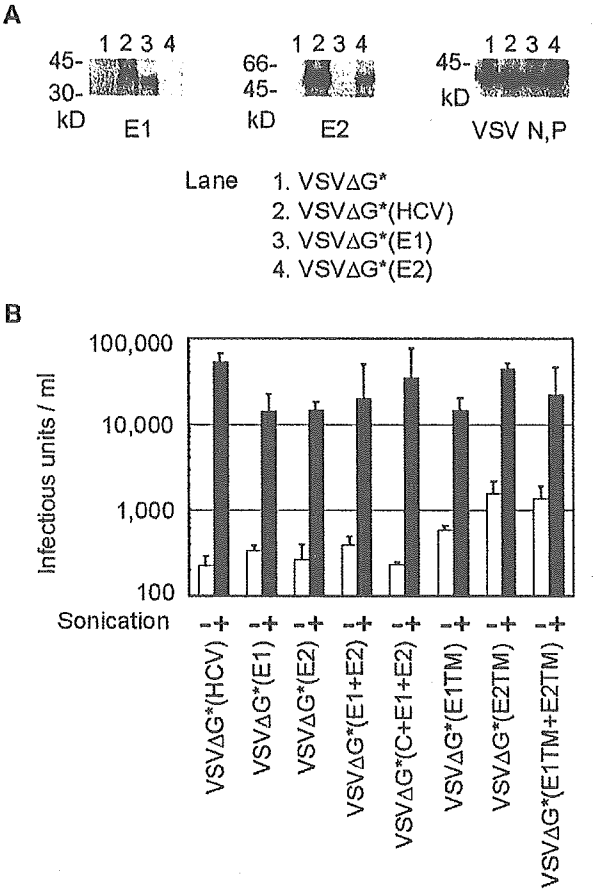

Fig. 2. (a) Western blot analyses of the pseudotype VSVs bearing HCV envelope proteins. Immunoblots of pseudotype virus samples through 20% sucrose cushions are shown. The preparation of each pseudotype sample is described in Table 2. E1 and E2 glycoproteins were detected with E1-384 and Mo-12 monoclonal antibodies against E1 [26] and E2 [27], respectively. VSV proteins were detected by polyclonal goat antibody. The positions of the molecular mass markers (kDa) are shown. (b) Effect of sonication on HCV pseudotype detection. VSV pseudotypes complemented with HCV envelope proteins were prepared after sonication (+, filled column) or without sonication (–, open column). HepG2 cells were infected with the indicated pseudotype viruses, and the IU were determined using the number of GFP-positive cells detected after 24 h of incubation.

faster than E2 reported in other studies [7,16]; this may be due to a variation in glycosylation of E2 among different HCV strains [31,34]. E1 and E2 bands were also detected in VSVΔG*(E1 + E2) or VSVΔG*(C + E1 + E2) samples (data not shown). Bands for the VSV structural proteins N and P with similar intensities were detected in all the four purified pseudotype samples by Western blotting, indicating that similar amounts of VSV were present there. As a control, 293T cells were transfected with E1 and/or E2 vectors but were not infected with VSVΔG*G later. Culture supernatants and cells were harvested, sonicated and subjected to ultracentrifugation, as described above. This sample was also analyzed by Western blotting, and neither E1 nor E2 was detected (data not shown). All these findings suggested the incorporation of the native forms of E1 and/or E2 into VSVΔG* viral particles.

Table 2
Designation of VSV pseudotype samples complemented with HCV glycoproteins

Pseudotype sample[a]	Plasmids
VSVΔG*G	pCAGGS/VSV-G
VSVΔG*(HCV)	pCXbsr/CE1E2
VSVΔG*(E1)	pCXbsr/E1
VSVΔG*(E2)	pCXbsr/E2
VSVΔG*(E1 + E2)	pCXbsr/E1 and pCXbsr/E2
VSVΔG*(C + E1 + E2)	pCXbsr/E1, pCXbsr/E2 and pCXbsr/C
VSVΔG*(E1TM)	pCXbsr/E1TM
VSVΔG*(E2TM)	pCXbsr/E2TM
VSVΔG*(E1TM + E2TM)	pCXbsr/E1TM and pCXbsr/E2TM
VSVΔG*[b]	PCXbsr

[a] VSV pseudotype samples were generated by transfection of cells with the indicated plasmids (total amount of DNA 2 μg per dish) and then by infection of the cells with VSVΔG*G 2 days later. Culture supernatants and the cells were harvested on the following day to prepare pseudotype samples, and stocked at –80 °C after sonication.

[b] VSVΔG* was recovered from cells transfected with pCXbsr plasmid containing no envelope glycoprotein.

3.2.2. *Effect of sonication on pseudotype virus preparation*

Next, we infected HepG2 cells with pseudotype samples that had been prepared with or without sonication. A large number of cells expressed GFP when the cells had been infected with the sonicated sample designated VSVΔG*(HCV), although much fewer cells expressed GFP when infected with the non-sonicated VSVΔG*(HCV) sample (Fig. 2b). The infectivities of other samples, i.e. VSVΔG*(E1), VSVΔG*(E2), VSVΔG*(E1 + E2), VSVΔG*(C + E1 + E2), VSVΔG*(E1TM), VSVΔG*(E2TM) and VSVΔG*(E1TM + E2TM), shown in Table 2, were also examined. The sonication procedure also enhanced their infectivities, as shown in Fig. 2b. In general, the infectivities of the virus samples that could bear the native forms of HCV envelope proteins were enhanced about 100-fold by sonication. With regard to VSVΔG*(E1TM), VSVΔG*(E2TM) and VSVΔG*(E1TM + E2TM), sonication enhanced these pseudotype titers about 10-fold (Fig. 2b).

3.3. *Neutralization of the pseudotype viruses*

To ascertain whether the infectivity of the VSV samples that could contain VSV pseudotypes was specific for the HCV envelope proteins, we examined whether the pseudotype virus activities could be inhibited by treatment with human sera as well as with bovine lactoferrin. While the anti-VSV antibody neutralized VSVΔG*G completely, it did not affect infection with VSVΔG*(HCV) at all (Fig. 3a). Infections of the other HCV pseudotype viruses were not affected by anti-VSV either (data not shown). These results suggested that the HCV envelope proteins conferred envelopes for VSVΔG*. None of the serum samples from 20 chronically HCV-infected Japanese patients, however, exhibited significant neutralization of HCV (E1E2), E1, or E2 pseudotype virus (data not shown). Previously, it was reported that serum samples from a majority of patients with chronic HCV infection failed to show detectable neutralization activity [19].

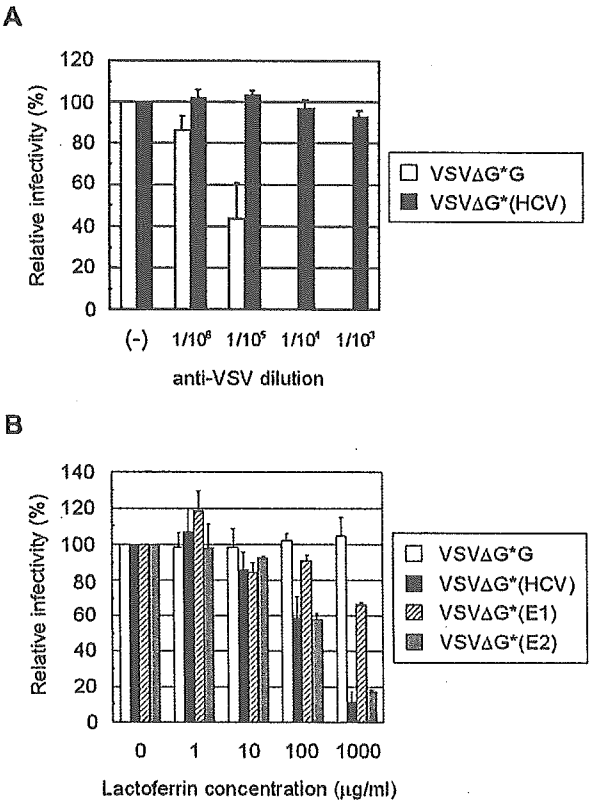

Fig. 3. (a) Neutralization of the pseudotype viruses. Two hundred IU of VSVΔG*(HCV) and VSVΔG*G was preincubated with the indicated dilutions of polyclonal antibody against VSV for 30 min and then inoculated to HepG2 cells. (b) Effect of bovine lactoferrin on the infectivity of pseudotype viruses. Each pseudotype virus (400 IU) was preincubated with various concentrations of bovine lactoferrin for 1 h and then inoculated to HepG2 cells for 1.5 h. Subsequently, the cells were washed with DMEM three times and maintained in culture medium. After 24 h of incubation, relative infectivity (%) was calculated by counting GFP-positive cells. The experiment was done in triplicate, and mean ± S.D. are shown.

3.4. *Effect of bovine lactoferrin on the infectivity of the pseudotype viruses*

We have reported, using PCR, that bovine lactoferrin prevents HCV infection in vitro [20,21]. As HCV-positive human sera were ineffective in inhibiting infection, to support the notion that HCV envelope-specific pseudotypes were formed, we examined whether we could show a specific interaction between lactoferrin and HCV pseudotype samples. Namely, each pseudotype sample was preincubated with various concentrations of lactoferrin, and then HepG2 cells were infected with them. The infectivities of the VSVΔG*(HCV) and VSVΔG*(E2) samples were reduced by preincubation with bovine lactoferrin in a dose-dependent manner, whereas VSVΔG*G was not inhibited (Fig. 3b). VSVΔG*(E1) was only slightly inhibited. This finding is consistent with the report that lactoferrin binds more specifically to E2 than E1 [35].

3.5. Susceptibility of various human cell lines to HCV pseudotypes

Next, we examined the susceptibility of various cell lines to the VSVΔG*(HCV) sample, using VSVΔG*G or VSVΔG* as a control (Table 3). VSVΔG* was prepared without supplying any envelope proteins and showed hardly any infectious titers. Hepatic cell lines, such as HepG2 and Huh7 cells, as well as 293T cells, showed a high susceptibility, and PH5CH8 cells showed a moderate susceptibility to VSVΔG*(HCV). Brain tumor-derived cell lines and primary brain-derived cells were moderately susceptible. Most hematopoietic cell lines were completely resistant to the pseudotype, while MT-2, a human T-cell leukemia virus type I (HTLV-I)-infected T cell line, and HEL, a human erythroleukemia cell line, showed a marginal susceptibility. MT-2 cells as well as HepG2 and PH5CH8 cells that have been reported to be susceptible to HCV infection [36] were susceptible to the VSVΔG*(HCV) sample, suggesting that VSV pseudotypes bearing HCV envelopes were formed.

The susceptibility of various types of cells shown in Table 3 to VSVΔG*(C + E1 + E2) or VSVΔG*(E1TM + E2TM) was also examined comparatively (Table 4). In hepatic cell lines, VSVΔG*(C + E1 + E2) and VSVΔG*(E1TM + E2TM) were nearly as infectious as VSVΔG*(HCV). Onto non-hepatic cells such as 293T, HBMEC or MT-2, VSVΔG*(HCV) plated

Table 3
Infectivity of pseudotype viruses in various human cells

Target	Origin	Pseudotype virus[a]			
		VSVΔG*(HCV)		VSVΔG*G	VSVΔG*
		IU/ml[b]	Ratio[c]	IU/ml	IU/ml
HepG2	Hepatoblastoma	53,000	1	3.4×10^8	280
Huh7	Hepatoma	25,000	0.47	1.2×10^9	1200
PH5CH8	Liver	4700	0.09	2.8×10^8	<10
293T	Embryonal kidney	50,000	0.94	6.8×10^8	300
HUK-1	Kidney	800	0.02	7.2×10^{10}	40
A172	Glioma	19,000	0.36	1.3×10^8	80
NP2	Glioma	15,000	0.28	2.6×10^8	<10
U251	Glioma	2200	0.04	1.1×10^9	<10
U87MG	Glioblastoma	1100	0.02	9.8×10^7	120
HBMEC	Brain microvascular endothelial cell	3600	0.07	3.1×10^8	100
HBP	Brain pericyte	520	0.01	2.8×10^7	60
HOS	Osteosarcoma	1500	0.03	1.0×10^7	20
Molt-4	T-cell acute lymphocytic leukemia	<10		1.2×10^9	<10
TALL-1	T-cell acute lymphocytic leukemia	40		3.2×10^8	<10
C8166	HTLV-1 (+) T cells	<10		8.0×10^8	<10
C91/PL	HTLV-1 (+) T cells	<10		2.0×10^8	100
MT-2	HTLV-1 (+) T cells	260	0.005	8.0×10^8	<10
BALL-1	B-cell acute lymphocytic leukemia	<10		1.7×10^8	<10
Daudi	Burkitt's lymphoma	<10		4.2×10^8	<10
Raji	Burkitt's lymphoma	<10		3.6×10^8	<10
Wil2NS	Plasmacytoma	20		5.2×10^8	<10
HEL	Erythroleukemia	240	0.005	1.4×10^9	<10
K562	Chronic myelogenous leukemia	40		2.8×10^8	20
HL-60	Acute promyelocytic leukemia	<10		4.2×10^7	20
U937	Histiocytic leukemia	<10		6.1×10^8	<10

[a] Pseudotype virus samples described in Table 2 were diluted and inoculated onto the indicated cells.
[b] Infectious units/ml (IU/ml) were determined by counting the number of GFP-expressing cells under a fluorescence microscope after 24 h infection. The experiments were done in triplicate, and means are shown.
[c] The relative ratio of infectious titers compared to HepG2 cells are shown.

Table 4
Infectivity of various HCV pseudotype viruses in human cells

Pseudotype virus[a]	IU/ml	Relative infectivity							
	HepG2	HepG2	Huh7	PH5CH8	293T	A172	NP2	HBMEC	MT-2
VSVΔG*(HCV)	53,000[b]	1[c]	0.47	0.09	0.94	0.36	0.28	0.07	0.005
VSVΔG*(C + E1 + E2)	35,000	1	0.40	0.05	0.45	0.19	0.10	0.01	0.001
VSVΔG*(E1TM + E2TM)	22,000	1	0.50	0.09	0.68	0.30	0.20	0.01	<0.001

The experiments were done in triplicate, and means are shown.
[a] Pseudotype virus samples described in Table 2 were diluted and inoculated onto the indicated cells.
[b] Infectious units/ml (IU/ml) were determined by counting the number of GFP-expressing cells under a fluorescence microscope after 24 h infection.
[c] The relative ratios of infectious titers to HepG2 cells are shown.

much more efficiently than VSVΔG*(C + E1 + E2) and VSVΔG*(E1TM + E2TM): these two latter pseudotypes were prepared with E1 and E2 expressed in *trans*.

3.6. Effect of sulfated polysaccharides on pseudotype virus infection

The infection of several flaviviruses, such as Japanese encephalitis virus and dengue virus serotype 2, has been reported to be inhibited by sulfated polysaccharides, especially heparan sulfate [37,38]. To investigate whether proteoglycans are involved in HCV infection, we examined the plating of VSVΔG*(HCV) and VSVΔG*G on HepG2 cells treated with heparitinase. Fig. 4a shows that heparitinase treatment of the cells reduced the plating of VSVΔG*(HCV). Next, we examined effects of highly sulfated polysaccharides, heparin, dextran sulfate (MW 8000 or 500,000), and unsulfated dextran (MW 7000) on VSVΔG*(HCV) infection (Fig. 4b). Heparin and sulfated dextrans effectively blocked VSVΔG*(HCV) infection, while unsulfated dextran was completely inactive in inhibiting VSVΔG*(HCV) infection. In contrast, the infectivity of VSVΔG*G was hardly affected by sulfated polysaccharides (data not shown).

To examine whether the sulfation level affected VSVΔG*(HCV) infection, sodium chlorate-treated HepG2 cells were infected with VSVΔG*(HCV), because sodium chlorate acts as a sulfate analog and reduces the sulfation level of cellular proteins and glycosaminoglycans (GAGs) [39,40]. Treatment of HepG2 cells with sodium chlorate reduced the VSVΔG*(HCV) titer by about 50% (data not shown). These results suggested that highly sulfated forms of the cell surface GAGs play roles in VSVΔG*(HCV) infection.

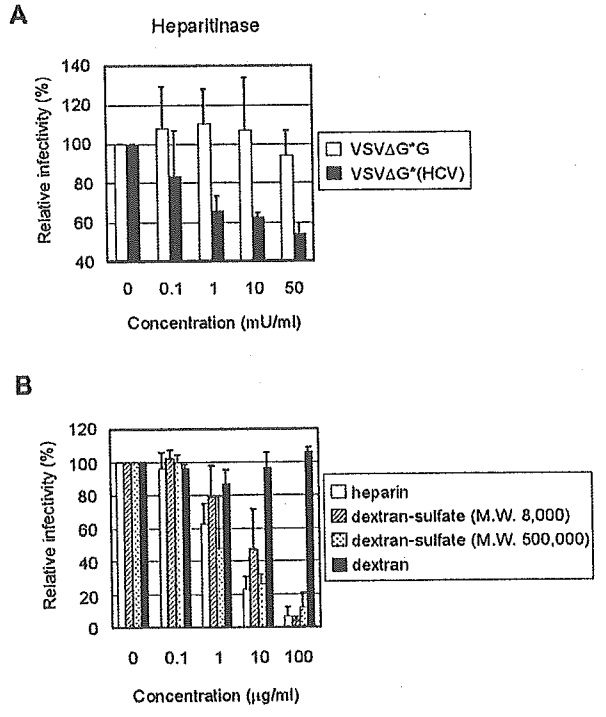

Fig. 4. Effects of sulfated polysaccharides on pseudotype infection. (a) Effect of heparitinase on infectivity of VSVΔG*(HCV). HepG2 cells were treated with various concentrations of heparitinase. The treated cells were infected with 200 IU of VSVΔG*(HCV) or VSVΔG*G. (b) Effect of sulfated polysaccharides on the infectivity of VSVΔG*(HCV). Two hundred IU of VSVΔG*(HCV) was preincubated with heparin, dextran sulfate or dextran at various concentrations for 1 h and then inoculated to HepG2 cells. After 24 h of incubation, the infectivity of the viruses was evaluated. The experiment was done in triplicate, and mean ± S.D. are shown.

3.7. Effects of enzymatic or chemical modification of the target cells on the plating of the HCV pseudotype

To characterize cellular factors necessary for HCV entry, we examined the plating of VSVΔG*(HCV) on HepG2 cells treated with various chemicals. Trypsin treatment of cells markedly reduced the infectivity of VSVΔG*(HCV), while the infectivity of VSVΔG*G was weakly affected (Fig. 5a). Either phospholipase C or sodium periodate marginally reduced the infectivity of VSVΔG*(HCV) (data not shown). Similar results were obtained with 293T cells (data not shown).

Next, the infection of VSVΔG*(HCV) was assessed with inhibitors of protein glycosylation. As shown in Fig. 5b, tunicamycin reduced the plating of VSVΔG*(HCV) by about 90%, whereas castanospermine reduced the infectivity by 20–30%, and neither deoxymannojirimycin nor swainsonine inhibited the plating of VSVΔG*(HCV) (data not shown). α-Mannosidase treatment of cells before infection reduced the infectivity of VSVΔG*(HCV) by about 70% at 500 μg/ml (Fig. 5c). These findings suggested that N-linked glycosylation of a protein(s) on the cell surface might have a role in HCV entry.

4. Discussion

We tried to develop a system to detect the infectivity of recombinant VSV pseudotypes bearing the native forms of HCV envelopes. The co-expression of E1 and E2, or expression of E1 or E2 alone, efficiently complemented the infectivity of VSV lacking the envelope G protein. We used the native forms of the HCV envelope proteins, because we considered that it might be more relevant to examine functions of the HCV envelopes. This system would enable us to study the early stages of HCV infection easily.

There has been no assay system in which infection of HCV has been detected readily and rapidly. For this, VSV pseudotype systems for HCV have been developed by several groups. Because both HCV E1 and E2 have ER retention signals in their C-terminal transmembrane domains, these proteins have been found to be retained in the ER [28–30]. This finding was confirmed by us (Table 1). Therefore, to prepare VSV pseudotypes bearing HCV envelopes, chimeric proteins consisting of carboxy-terminal-truncated HCV envelopes fused to the transmembrane and cytoplasmic tail of VSV G glycoprotein have been used to localize them on the cell surface [15–17]. Baumert et al. [41] reported that HCV-like particle

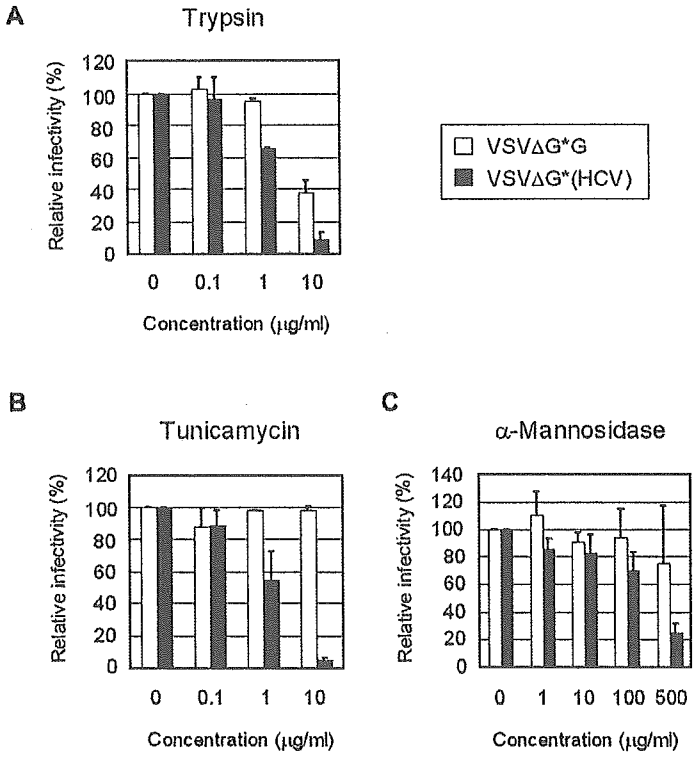

Fig. 5. Infectivity of pseudotype viruses in chemically modified cells. (a) HepG2 cells were preincubated with various concentrations of trypsin for 5 min. Subsequently, an equal volume of complete medium was added to stop the enzyme. Then, the cells were washed and infected with 200 IU of each virus. (b) Effect of glycosylation of cell surface components on the infectivity of VSVΔG*(HCV). HepG2 cells were preincubated with the indicated concentrations of tunicamycin for 24 h. Then, the cells were infected with 200 IU of each virus. (c) Effect of α-mannosidase treatment of cells on the entry of VSVΔG*(HCV). HepG2 cells were preincubated with α-mannosidase at various concentrations for 1 h. Then, the cells were washed and infected with 200 IU of each virus. After 24 h of incubation, the infectivity of the viruses was determined. The experiment was done in triplicate, and mean ± S.D. are shown.

assembly occurs in the cytoplasmic vesicles and that pseudoparticles bearing native HCV envelope proteins will not be released or secreted into culture medium, but accumulate in the ER, like parental HCV virions. There is, however, a possibility that these VSV pseudotype viruses might not exactly reflect the characteristics of the native envelope proteins of viral particles.

HCV virions bearing the native form of HCV envelope proteins should be released from cells in vivo, since plasma samples of HCV-infected humans have frequently shown high infectivity [1,5,42]. It is enigmatic for us how HCV virions have been produced in vivo; nevertheless, both E1 and E2 proteins harbor the ER retention signal. Very recently, Bartosch et al. [43] and Hsu et al. [44] reported the existence of pseudoparticles bearing unmodified HCV envelopes on retroviral core particles. They suggested that a small portion of E1 and E2 would be expressed on the cell surface when these proteins had been expressed abundantly in cells, and thus the retroviral pseudotype bearing E1E2 could be detected. In contrast, we showed that VSV pseudotypes bearing the native form of HCV envelope proteins with highly infectious titers, as compared with previous reports, could be produced by the cells expressing the HCV envelope proteins in the cytoplasm (Table 1 and Fig. 2).

Unlike previous studies [15–17], we thus successfully detected the infectious activities considered to be due to the formation of VSV pseudotype viruses when VSV was complemented with the native forms of HCV envelope proteins. Although only a small amount of pseudotype virus was initially detected in the culture medium, when the harvested pseudotype samples were sonicated for a short time, their titers were enhanced about 100-fold (Fig. 2b). In our assay system, the carryover of VSVΔG*G into HCV pseudotype samples would be minimized by treatment with polyclonal antibody to VSV. Probably due to the efficient decrease in the carryover and the release of pseudotype virions associated with the cell membrane by sonication, we could detect HCV pseudotypes with the native forms of envelopes.

We have reported that bovine and human lactoferrins prevent HCV infection in PH5CH8 human liver cells and MT-2 cells [20,21], and HCV E1 and E2 bind to lactoferrin [35]. We have also reported that the lactoferrin-binding activity of E2 contributes to inhibition of HCV infection [45]. In the present study, pretreatment of VSV pseudotypes with bovine lactoferrin reduced the infectivity of VSVΔG*(HCV) and VSVΔG*(E2) in a dose-dependent manner, whereas pretreatment with transferrin did not (data not shown). In contrast, lactoferrins partially inhibited the infectivity of VSVΔG*(E1) (Fig. 3b). Our results suggested that the interaction between lactoferrin and E2 plays a central role in the inhibition of HCV infection. Taken together, our findings

showed that properties of HCV pseudotypes are consistent with those of HCV virions determined by PCR.

Previously, several groups have demonstrated that not only human hepatic cell lines but also human T cell lines, Molt-4Ma, HPB-Ma, MT-2, and a human B cell line, Daudi, are susceptible to HCV infection [46–49]. In the present study, almost no hematopoietic cell lines were susceptible to any HCV pseudotypes. Only MT-2 and HEL cells showed a marginal susceptibility to the HCV pseudotypes. It is probable that the characteristics of the cell lines might change after long-term cell culture in different laboratories. Interestingly, our results demonstrated that several cell lines derived from the human brain were apparently susceptible to HCV pseudotypes. Encephalomyelitis or encephalitis associated with HCV and cerebral involvement of HCV infection have been reported [50–52]; HCV RNA has been detected in the post-mortem brain and brainstem [53].

Weak immunity against HCV infection has been reported [54]. Recently, it has been documented that serum samples from a majority of patients with chronic HCV infection failed to show a detectable neutralization activity against VSV pseudotypes bearing chimeric HCV envelopes [19]. Also in our study, no significant neutralization of any HCV pseudotypes was observed with serum samples from 20 patients with chronic HCV infection. It should be determined whether neutralizing antibody against E1 or E2 alone can neutralize the VSVΔG*(HCV) pseudotype. If E1 and E2 can function independently and the neutralization of both E1 and E2 is necessary for marked inhibition of HCV infectivity, the development of an effective vaccine or an HCV entry-inhibiting agent will be quite difficult. For detection of neutralizing antibody, it may be necessary to examine patients at the different stages of HCV infection, e.g. acute stage of hepatitis.

Table 4 shows that the three different types of HCV pseudotypes prepared with two HCV envelopes showed only a small difference in infectivity in eight types of cells. As for the difference in infectivity between VSVΔG*(HCV) prepared with structural proteins in *cis* and VSVΔG*(C + E1 + E2) prepared with structural proteins in *trans*, it might be explained by the difference in E1–E2 interaction between them. There are reports that both E1 and E2 are necessary for the efficient formation of VSV or retroviral pseudotypes [17,43,44], while VSV pseudotypes complemented with either E1 or E2 alone have been developed [16]. Our findings also suggest that either E1 or E2 alone is enough to make HCV virions (Fig. 2). Recent study indicates that the presence of the complete HCV core sequence is crucial for the expression and/or post-translational processing of the complex-type glycosylated form of E2 [34], and the glycosylation of E1 is enhanced by coexpression of E2 in *cis* [33]. Our results indicate that the core protein might be required for maximal infectivity of pseudotypes (Fig. 2b). Further studies are needed to clarify the role of each envelope protein in the infection by HCV.

Many viruses including herpes viruses, human immunodeficiency virus, Sindbis virus, and in particular, flaviviruses such as dengue virus serotype 2 and Japanese encephalitis virus utilize proteoglycans, especially heparan sulfate, to mediate attachment to and infection of target cells [37,38,55–57]. Recently, Germi et al. [58] reported that cellular heparin-like GAGs might bind to HCV. Our results suggested that highly sulfated forms of GAGs play a role in the early stage of HCV infection (Fig. 4).

Assays of virus infectivity using chemically modified cells suggest that certain cell surface glycoproteins with N-linked oligosaccharides play an important role in VSVΔG*(HCV) infection (Fig. 5b). In addition, pre-treatment of cells with α-mannosidase suppressed the infectivity of VSVΔG*(HCV) by about 70% (Fig. 5c). Further studies on the surface sugar chain structures of cells will be needed to analyze their roles in the entry of HCV.

In conclusion, our system of producing VSV pseudotypes complemented with the native forms of HCV envelopes will be a useful tool with which to analyze the mechanism for HCV virion formation and the function of HCV envelope proteins. This system may also be an efficient tool for research on HCV entry and its inhibitors.

Acknowledgments

We thank Dr. M.A. Whitt for kindly supplying a VSV G-expressing pCAGGS/VSV-G plasmid and the VSVΔG*G pseudotype. We also thank Dr. M. Kohara for kindly providing us with anti-E1 monoclonal antibody. This work was supported in part by a grant-in-aid from the Japanese Society for the Promotion of Science, grants from the Japan Health Sciences Foundation and CREST, and the 21st century COE program.

References

[1] H.J. Alter, R.H. Purcell, J.W. Shih, J.C. Melpolder, M. Houghton, Q.L. Choo, et al., Detection of antibody to hepatitis C virus in prospectively followed transfusion recipients with acute and chronic non-A, non-B hepatitis, N. Engl. J. Med. 321 (1989) 1494–1500.

[2] M.E. Major, B. Rehermann, S.M. Feinstone, in: D.M. Knipe, P.M. Howley (Eds.), Fields Virology, fourth ed, Lippincott, Philadelphia, PA, 2001, pp. 1127–1161.

[3] M.J. Alter, H.S. Margolis, K. Krawczynski, F.N. Judson, A. Mares, W.J. Alexander, et al., The natural history of community-acquired hepatitis C in the United States, N. Engl. J. Med. 327 (1992) 1899–1905.

[4] I. Saito, T. Miyamura, A. Ohbayashi, H. Harada, T. Katayama, S. Kikuchi, et al., Hepatitis C virus infection is associated with the development of hepatocellular carcinoma, Proc. Natl. Acad. Sci. USA 87 (1990) 6547–6549.

[5] Q.L. Choo, G. Kuo, A.J. Weiner, L.R. Overby, D.W. Bradley, M. Houghton, Isolation of a cDNA clone derived from a blood-borne non-A, non-B viral hepatitis genome, Science 244 (1989) 359–362.

[6] N. Kato, M. Hijikata, Y. Ootsuyama, M. Nakagawa, S. Ohkoshi, T. Sugimura, et al., Molecular cloning of the human hepatitis C virus genome from Japanese patients with non-A, non-B hepatitis, Proc. Natl. Acad. Sci. USA 87 (1990) 9524–9528.

[7] A. Grakoui, C. Wychowski, C. Lin, S.M. Feinstone, C.M. Rice, Expression and identification of hepatitis C virus polyprotein cleavage products, J. Virol. 67 (1993) 1385–1395.
[8] M.J. Selby, Q.L. Choo, K. Berger, G. Kuo, E. Glazer, M. Eckart, et al., Expression, identification and subcellular localization of the proteins encoded by the hepatitis C viral genome, J. Gen. Virol. 74 (1993) 1103–1113.
[9] V. Deleersnyder, A. Pillez, C. Wychowski, K. Blight, J. Xu, Y.S. Hahn, et al., Formation of native hepatitis C virus glycoprotein complexes, J. Virol. 71 (1997) 697–704.
[10] P. Pileri, Y. Uematsu, S. Campagnoli, G. Galli, F. Falugi, R. Petracca, et al., Binding of hepatitis C virus to CD81, Science 282 (1998) 938–941.
[11] E. Scarselli, H. Ansuini, R. Cerino, R.M. Roccasecca, S. Acali, G. Filocamo, C. Traboni, A. Nicosia, R. Cortese, A. Vitelli, The human scavenger receptor class B type I is a novel candidate receptor for the hepatitis C virus, EMBO J. 21 (2002) 5017–5025.
[12] V. Agnello, G. Abel, M. Elfahal, G.B. Knight, Q.X. Zhang, Hepatitis C virus and other flaviviridae viruses enter cells via low density lipoprotein receptor, Proc. Natl. Acad. Sci. USA 96 (1999) 12766–12771.
[13] S. Wunschmann, J.D. Medh, D. Klinzmann, W.N. Schmidt, J.T. Stapleton, Characterization of hepatitis C virus (HCV) and HCV E2 interactions with CD81 and the low-density lipoprotein receptor, J. Virol. 74 (2000) 10055–10062.
[14] F. Masciopinto, G. Freer, V.L. Burgio, S. Levy, L. Galli-Stampino, M. Bendinelli, M. Houghton, S. Abrignani, Y. Uematsu, Expression of human CD81 in transgenic mice does not confer susceptibility to hepatitis C virus infection, Virology 304 (2002) 187–196.
[15] L. Buonocore, K.J. Blight, C.M. Rice, J.K. Rose, Characterization of vesicular stomatitis virus recombinants that express and incorporate high levels of hepatitis C virus glycoproteins, J. Virol. 76 (2002) 6865–6872.
[16] L.M. Lagging, K. Meyer, R.J. Owens, R. Ray, Functional role of hepatitis C virus chimeric glycoproteins in the infectivity of pseudotyped virus, J. Virol. 72 (1998) 3539–3546.
[17] Y. Matsuura, H. Tani, K. Suzuki, T.S. Kimura, R. Suzuki, H. Aizaki, K. Ishii, K. Moriishi, C.S. Robison, M.A. Whitt, T. Miyamura, Characterization of pseudotype VSV possessing HCV envelope proteins, Virology 286 (2001) 263–275.
[18] A. Takada, C. Robison, H. Goto, A. Sanchez, K.G. Murti, M.A. Whitt, et al., A system for functional analysis of Ebola virus glycoprotein, Proc. Natl. Acad. Sci. USA 94 (1997) 14764–14769.
[19] L.M. Lagging, K. Meyer, J. Westin, R. Wejstal, G. Norkrans, M. Lindh, R. Ray, Neutralization of pseudotyped vesicular stomatitis virus expressing hepatitis C virus envelope glycoprotein 1 or 2 by serum from patients, J. Infect. Dis. 185 (2002) 1165–1169.
[20] M. Ikeda, K. Sugiyama, T. Tanaka, K. Tanaka, H. Sekihara, K. Shimotohno, et al., Lactoferrin markedly inhibits hepatitis C virus infection in cultured human hepatocytes, Biochem. Biophys. Res. Commun. 245 (1998) 549–553.
[21] M. Ikeda, A. Nozaki, K. Sugiyama, T. Tanaka, A. Naganuma, K. Tanaka, et al., Characterization of antiviral activity of lactoferrin against hepatitis C virus infection in human cultured cells, Virus Res. 66 (2000) 51–63.
[22] R.B. DuBridge, P. Tang, H.C. Hsia, P.M. Leong, J.H. Miller, M.P. Calos, Analysis of mutation in human cells by using an Epstein–Barr virus shuttle system, Mol. Cell. Biol. 7 (1987) 379–387.
[23] M. Ikeda, K. Sugiyama, T. Mizutani, T. Tanaka, K. Tanaka, H. Sekihara, et al., Human hepatocyte clonal cell lines that support persistent replication of hepatitis C virus, Virus Res. 56 (1998) 157–167.
[24] T. Akagi, T. Shishido, K. Murata, H. Hanafusa, v-Crk activates the phosphoinositide 3-kinase/AKT pathway in transformation, Proc. Natl. Acad. Sci. USA 97 (2000) 7290–7295.
[25] H. Niwa, K. Yamamura, J. Miyazaki, Efficient selection for high-expression transfectants with a novel eukaryotic vector, Gene 108 (1991) 193–199.
[26] T. Wakita, C. Taya, A. Katsume, J. Kato, H. Yonekawa, Y. Kanegae, et al., Efficient conditional transgene expression in hepatitis C virus cDNA transgenic mice mediated by the cre/loxP system, J. Biol. Chem. 273 (1998) 9001–9006.
[27] M. Inudoh, N. Kato, Y. Tanaka, New monoclonal antibodies against a recombinant second envelope protein of hepatitis C virus, Microbiol. Immunol. 42 (1998) 875–877.
[28] L. Cocquerel, J.C. Meunier, A. Pillez, C. Wychowski, J. Dubuisson, A retention signal necessary and sufficient for endoplasmic reticulum localization maps to the transmembrane domain of hepatitis C virus glycoprotein E2, J. Virol. 72 (1998) 2183–2191.
[29] L. Cocquerel, S. Duvet, J.C. Meunier, A. Pillez, R. Cacan, C. Wychowski, et al., The transmembrane domain of hepatitis C virus glycoprotein E1 is a signal for static retention in the endoplasmic reticulum, J. Virol. 73 (1999) 2641–2649.
[30] L. Cocquerel, C. Wychowski, F. Minner, F. Penin, J. Dubuisson, Charged residues in the transmembrane domains of hepatitis C virus glycoproteins play a major role in the processing, subcellular localization, and assembly of these envelope proteins, J. Virol. 74 (2000) 3623–3633.
[31] H.J. Ezelle, D. Markovic, G.N. Barber, Generation of hepatitis C virus-like particles by use of a recombinant vesicular stomatitis virus vector, J. Virol. 76 (2002) 12325–12334.
[32] B. Bartosch, A. Vitelli, C. Granier, C. Goujon, J. Dubuisson, S. Pascale, E. Scarselli, R. Cortese, A. Nicosia, F.L. Cosset, Cell entry of hepatitis C virus requires a set of co-receptors that include the CD81 tetraspanin and the SR-IB scavenger receptor, J. Biol. Chem. 278 (2003) 41624–41630.
[33] A. Goffard, J. Dubuisson, Glycosylation of hepatitis C virus envelope proteins, Biochimie 85 (2003) 295–301.
[34] L.X. Zhu, L. Liu, Y.C. Li, Y.Y. Kong, C. Staib, G. Sutter, Y. Wang, G.D. Li, Full-length core sequence dependent complex-type glycosylation of hepatitis C virus E2 glycoprotein, World J. Gastroenterol. 8 (2002) 499–504.
[35] M. Yi, S. Kaneko, D.Y. Yu, S. Murakami, Hepatitis C virus envelope proteins bind lactoferrin, J. Virol. 71 (1997) 5997–6002.
[36] N. Kato, M. Ikeda, K. Sugiyama, T. Mizutani, T. Tanaka, K. Shimotohno, Hepatitis C virus population dynamics in human lymphocytes and hepatocytes infected in vitro, J. Gen. Virol. 79 (1998) 1859–1869.
[37] Y. Chen, T. Maguire, R.E. Hileman, J.R. Fromm, J.D. Esko, R.J. Linhardt, et al., Dengue virus infectivity depends on envelope protein binding to target cell heparan sulfate, Nat. Med. 3 (1997) 866–871.
[38] C.M. Su, C.L. Liao, Y.L. Lee, Y.L. Lin, Highly sulfated forms of heparin sulfate are involved in Japanese encephalitis virus infection, Virology 286 (2001) 206–215.
[39] P.A. Baeuerle, W.B. Huttner, Chlorate—a potent inhibitor of protein sulfation in intact cells, Biochem. Biophys. Res. Commun. 141 (1986) 870–877.
[40] F. Safaiyan, S.O. Kolset, K. Prydz, E. Gottfridsson, U. Lindahl, M. Salmivirta, Selective effects of sodium chlorate treatment on the sulfation of heparan sulfate, J. Biol. Chem. 274 (1999) 36267–36273.
[41] T.F. Baumert, S. Ito, D.T. Wong, T.J. Liang, Hepatitis C virus structural proteins assemble viruslike particles in insect cells, J. Virol. 72 (1998) 3827–3836.
[42] G. Kuo, Q.L. Choo, H.J. Alter, G.L. Gitnick, A.G. Redeker, R.H. Purcell, et al., An assay for circulating antibodies to a major etiologic virus of human non-A, non-B hepatitis, Science 244 (1989) 362–364.
[43] B. Bartosch, J. Dubuisson, F.L. Cosset, Infectious hepatitis C virus pseudo-particles containing functional E1–E2 envelope protein complexes, J. Exp. Med. 197 (2003) 633–642.
[44] M. Hsu, J. Zhang, M. Flint, C. Logvinoff, C.C. Mayer, C.M. Rice, J.A. McKeating, Hepatitis C virus glycoproteins mediate pH-dependent cell entry of pseudotyped retroviral particles, Proc. Natl. Acad. Sci. USA 100 (2003) 7271–7276.
[45] A. Nozaki, M. Ikeda, A. Naganuma, T. Nakamura, M. Inudoh, K. Tanaka, N. Kato, Identification of a lactoferrin-derived peptide possessing binding activity to hepatitis C virus E2 envelope protein, J. Biol. Chem. 278 (2003) 10162–10173.

[46] T. Mizutani, N. Kato, S. Saito, M. Ikeda, K. Sugiyama, K. Shimotohno, Characterization of hepatitis C virus replication in cloned cells obtained from a human T-cell leukemia virus type 1-infected cell line, MT-2, J. Virol. 70 (1996) 7219–7223.

[47] N. Nakajima, M. Hijikata, H. Yoshikura, Y.K. Shimizu, Characterization of long-term cultures of hepatitis C virus, J. Virol. 70 (1996) 3325–3329.

[48] Y.K. Shimizu, A. Iwamoto, M. Hijikata, R.H. Purcell, H. Yoshikura, Evidence for in vitro replication of hepatitis C virus genome in a human T-cell line, Proc. Natl. Acad. Sci. USA 89 (1992) 5477–5481.

[49] Y.K. Shimizu, R.H. Purcell, H. Yoshikura, Correlation between the infectivity of hepatitis C virus in vivo and its infectivity in vitro, Proc. Natl. Acad. Sci. USA 90 (1993) 6037–6041.

[50] D.M. Forton, J.M. Allsop, J. Main, G.R. Foster, H.C. Thomas, S.D. Taylor-Robinson, Evidence for a cerebral effect of the hepatitis C virus, Lancet 358 (2001) 38–39.

[51] H. Fujita, Y. Chuganji, M. Yaginuma, M. Momoi, T. Tanaka, Case report: acute encephalitis immediately prior to acute onset of hepatitis C virus infection, J. Gastroenterol. Hepatol. 14 (1999) 1129–1131.

[52] S. Sacconi, S. Salviati, E. Merelli, Acute disseminated encephalomyelitis associated with hepatitis C virus infection, Arch. Neurol. 58 (2001) 1679–1681.

[53] H. Bolay, F. Soylemezoglu, G. Nurlu, S. Tuncer, K. Varli, PCR detected hepatitis C virus genome in the brain of a case with progressive encephalomyelitis with rigidity, Clin. Neurol. Neurosurg. 98 (1996) 305–308.

[54] A.M. Prince, B. Brotman, T. Huima, D. Pascual, M. Jaffery, G. Inchauspe, Immunity in hepatitis C infection, J. Infect. Dis. 165 (1992) 438–443.

[55] A.P. Byrnes, D.E. Griffin, Binding of sindbis virus to cell surface heparan sulfate, J. Virol. 72 (1998) 7349–7356.

[56] M. Moulard, H. Lortat-Jacob, I. Mondor, G. Roca, R. Wyatt, J. Sodroski, et al., Selective interactions of polyanions with basic surfaces on human immunodeficiency virus type 1 gp120, J. Virol. 74 (2000) 1948–1960.

[57] D. Shukla, J. Liu, P. Blaiklock, N.W. Shworak, X. Bai, J.D. Esko, et al., A novel role for 3-O-sulfated heparan sulfate in herpes simplex virus 1 entry, Cell 99 (1999) 13–22.

[58] R. Germi, J.M. Crance, D. Garin, J. Guimet, H. Lortat-Jacob, R.W.H. Ruigrok, et al., Cellular glycosaminoglycans and low density lipoprotein receptor are involved in hepatitis C virus adsorption, J. Med. Virol. 68 (1999) 206–215.

Available online at www.sciencedirect.com
SCIENCE DIRECT®
Virology 346 (2006) 348 – 362
VIROLOGY
www.elsevier.com/locate/yviro

Hepatitis C virus NS5B delays cell cycle progression by inducing interferon-β via Toll-like receptor 3 signaling pathway without replicating viral genomes

Kazuhito Naka [a,1], Hiromichi Dansako [a,1], Naoya Kobayashi [b], Masanori Ikeda [a], Nobuyuki Kato [a,*]

[a] *Department of Molecular Biology, Okayama University Graduate School of Medicine, Dentistry, and Pharmaceutical Sciences, 2-5-1 Shikata-cho, Okayama 700-8558, Japan*
[b] *Department of Surgery, Okayama University Graduate School of Medicine, Dentistry, and Pharmaceutical Sciences, 2-5-1 Shikata-cho, Okayama 700-8558, Japan*

Received 1 July 2005; returned to author for revision 11 August 2005; accepted 18 October 2005
Available online 2 December 2005

Abstract

To clarify the pathogenesis of hepatitis C virus (HCV), we have studied the effects of HCV proteins using human hepatocytes. Here, we found that HCV NS5B, an RNA-dependent RNA polymerase, delayed cell cycle progression through the S phase in PH5CH8 immortalized human hepatocyte cells. Since treatment with anti-interferon (IFN)-β neutralizing antibody restored the cell cycle delay, IFN-β was deemed responsible for the cell cycle delay in NS5B-expressing PH5CH8 cells. The induction of IFN-β and the cell cycle delay were overridden by the down-regulation of Toll-like receptor 3 (TLR3) through RNA interference in NS5B-expressing PH5CH8 cells. Moreover, the NS5B full form was required for the cell cycle delay, the induction of IFN-β, and the activation of the IFN-β signaling pathway. Our findings revealed that NS5B induced IFN-β through the TLR3 signaling pathway in immortalized human hepatocytes even without replicating viral genomes.

Keywords: Hepatitis C virus; NS5B; Interferon-β; TLR3; Hepatocyte cells

Introduction

Since more than 170 million individuals are estimated to be infected with hepatitis C virus (HCV) worldwide, this disease is a global health problem (Thomas, 2000). HCV belongs to the family Flaviviridae, whose positive-stranded RNA genome encodes a large polyprotein precursor of approximately 3000 amino acid residues. This polyprotein is processed by a combination of the host and viral proteases into at least ten proteins in the following order: NH_2-core-envelope 1-envelope 2-p7-nonstructural protein 2 (NS2)-NS3-NS4A-NS4B-NS5A-NS5B-COOH (Kato, 2001; Kato et al., 1990). These viral proteins are not only involved in viral replication but also may affect a variety of cellular functions (Bartenschlager and Lohmann, 2000; Kato, 2001). Although persistent infection with HCV is a major cause of chronic hepatitis, liver cirrhosis, and hepatocellular carcinoma (HCC) (Colombo, 1996; Kato, 2001), the molecular mechanisms leading to liver cell dysplasia and HCC remain elusive.

It has been thought that unregulated cell cycle progression may be a cause of malignant transformation of normal cells. On the other hand, inhibition of cell cycle progression through the S phase may cause replication error during DNA replication, which induces genomic instability and malignant transformation. Therefore, it is important to clarify the effect of HCV proteins on cell cycle progression in order to understand the molecular mechanism underlying the pathogenesis of HCV, including the development of HCC. A number of previous reports suggested that four HCV proteins—the core, NS3, NS4B, and NS5A—are involved in modulating cell cycle progression (Arima et al., 2001; Kato, 2001; Ray and Ray, 2001; Reed and Rice, 2000). For instance, the core protein promotes cell proliferation through the Ras/Raf signaling pathway and the anti-apoptotic function (Mar-

* Corresponding author. Fax: +81 86 235 7392.
E-mail address: nkato@md.okayama-u.ac.jp (N. Kato).
[1] Both authors contributed equally to this work.

0042-6822/$ - see front matter © 2005 Elsevier Inc. All rights reserved.
doi:10.1016/j.virol.2005.10.023

usawa et al., 1999; Tsuchihara et al., 1999). However, the core has been described to both enhance and repress the function of $p21^{Waf1/Cip1/Sdi1}$, a Cdk inhibitor (Dubourdeau et al., 2002; Jung et al., 2001; Lu et al., 1999; Ray et al., 1998). Recently, Scholle et al. found no significant cell cycle delay in human hepatoma HuH-7-based HCV RNA-replicating cells that were autonomously replicating genome-length HCV RNA, in comparison with cured cells of the same line from which HCV RNA had been eliminated by treatment with interferon (IFN)-α (Scholle et al., 2004). Hence, the effects of cell cycle regulation by HCV proteins are still controversial. Cancerous cell lines, such as the human hepatoma HuH-7 cell line (Hsu et al., 1993), which harbors a mutant *p53* gene, may not be suitable for addressing the effects of HCV proteins on cell cycle progression.

The PH5CH8 cell line was established by immortalization using the SV40 large-T antigen from non-neoplastic liver tissue of an HCV-related HCC patient (Ikeda et al., 1998; Noguchi and Hirohashi, 1996). PH5CH8 cells possess wild-type *p53* and *Rb* tumor suppressor genes. In nude mice, these cells reveal a non-malignant phenotype upon colony formation and tumorigenicity (Noguchi and Hirohashi, 1996), although the SV40 large-T antigen would partially repress the function of p53. Therefore, the PH5CH8 cell line is considered to be more relevant for studying the role of HCV proteins during hepatocarcinogenesis. We have previously reported that the HCV core protein activates the IFN-inducible 2′–5′-oligoadenylate synthetase gene in PH5CH8 cells (Naganuma et al., 2000). Recently, we demonstrated that the core protein's activation of this gene was mediated through the IFN-stimulated response element (ISRE) (Dansako et al., 2003). Furthermore, we found that the core protein promoted microsatellite instability in PH5CH8 cells (Naganuma et al., 2004). In fact, microsatellite instability was detected in approximately 20% of the tumor tissues from HCC patients examined, whereas no microsatellite instability was detected in normal liver tissues from the same patients (Dore et al., 2001; Kondo et al., 2000). In order to clarify the effect of HCV proteins on cell cycle progression in PH5CH8 cells, we examined cell cycle progression after the cells were released from the G1/S boundary in PH5CH8 cells expressing HCV proteins. We found that NS5B delays cell cycle progression by inducing IFN-β through the activation of the Toll-like receptor 3 (TLR3) signaling pathway without replicating viral genomes.

Results

HCV NS5B causes the delay of S phase progression

In a previous study of virus–host interactions, we examined whether or not HCV proteins affect cell cycle progression in PH5CH8 cells that stably expressed core or NS proteins. PH5CH8 cells were infected with retrovirus pCXbsr as a negative control (Ctr) or pCXbsr encoding either an HCV structural protein (HA-core) or NS protein (NS3, HA-NS4B, HA-NS5A, HA-NS5B, or NS5B), and we obtained PH5CH8 cells stably expressing each HCV protein. The expression of each HCV protein was confirmed by Western blot analysis (Fig. 1A). Then, the HCV protein-expressing cells were synchronized at the G1/S boundary, and cell cycle progression (from the S phase to the G2-M phase, then turning back to the G1 phase) was analyzed after the cells were released from synchronization. This cell cycle analysis revealed no significant differences in cell cycle progression between cells (PH/Ctr) infected with a control pCXbsr retrovirus and cells expressing core, NS3, NS4B, or NS5A (Fig. 1B). Unlike the PH/Ctr cells, the apparent delay of S phase progression was found in cells (PH/NS5B) expressing NS5B, regardless of the presence of the HA tag (Fig. 1B). To exclude the possibility that pCXbsr-derived retrovirus proteins synergistically affect the cell cycle together with NS5B, the retrovirus pCX4bsr vector (Akagi et al., 2003), which eliminates the production of any fusion proteins resulting from initiation at upstream AUG codons within the *gag* region of the vector, was used for the cell cycle analysis. As a result, the delay of S phase progression was found again in PH5CH8 cells expressing NS5B (Figs. 1A and C), suggesting that the retrovirus proteins are not involved in the delay of S phase progression. BrdUrd incorporation analysis was also carried out using PH/Ctr and PH/NS5B cells (Fig. 1D). In the PH/Ctr cells, DNA synthesis began early in the S phase (4 h after release). In the late S phase (8 h), more than 61% of the cells indicated final DNA synthesis. Thereafter, the cells either finished DNA replication in the G2-M phase (12 h) or returned to the G1 phase. In contrast, we found that DNA replication in most PH/NS5B cells predominantly remained in the early or middle S phase (8 h), and 49% of the cells were prolonged in the late S phase (12 h). To quantitatively evaluate this delay in S phase progression, the cells that had finished DNA replication were accumulated during the G2 phase by treatment with Nocodazole (Noc), which inhibits the progression of the G2 to M phases, after the cells were released from the G1/S transition. Whereas 77% of PH/Ctr cells reached the G2-M phase, only 37% of PH/NS5B cells did so (Fig. 1D). This level of decrease in cell numbers in the G2-M phase was not observed in PH5CH8 cells expressing core, NS3, NS4B, or NS5A (Fig. 1E), suggesting that NS5B specifically causes the delay of S phase progression in PH5CH8 cells. We further observed that the growth rate of PH/NS5B cells was significantly decreased relative to PH/Ctr cells (Fig. 1F), although the cell cycle distribution in asynchronous PH/NS5B cells was almost the same as that in asynchronous PH/Ctr cells (Fig. 1D). These results indicated that NS5B might delay the cell cycle progression of PH5CH8 cells in the S phase.

Cell cycle delay by NS5B is also found in other immortalized human hepatocytes

To clarify whether or not the delay of S phase progression by NS5B occurs in other human cell lines, we prepared three cell lines (Fig. 2A) that stably express NS5B–non-neoplastic human hepatocyte NKNT-3 (Kobayashi et al., 2000), hepatoma

HuH-7, and cervical carcinoma HeLa–and subjected them to the cell cycle analysis described above. The results revealed that S phase progression was delayed in NKNT-3, but not in HuH-7 or HeLa cells (Fig. 2B). This indicates that the delay of the cell cycle by NS5B expression is not limited to PH5CH8 cells.

IFN-β mediates the delay of S phase progression by NS5B

Since it has been reported previously that IFN-β induced the delay of S phase progression in human cultured cells (Vanmucchi et al., 2000), we speculated that IFN-β was

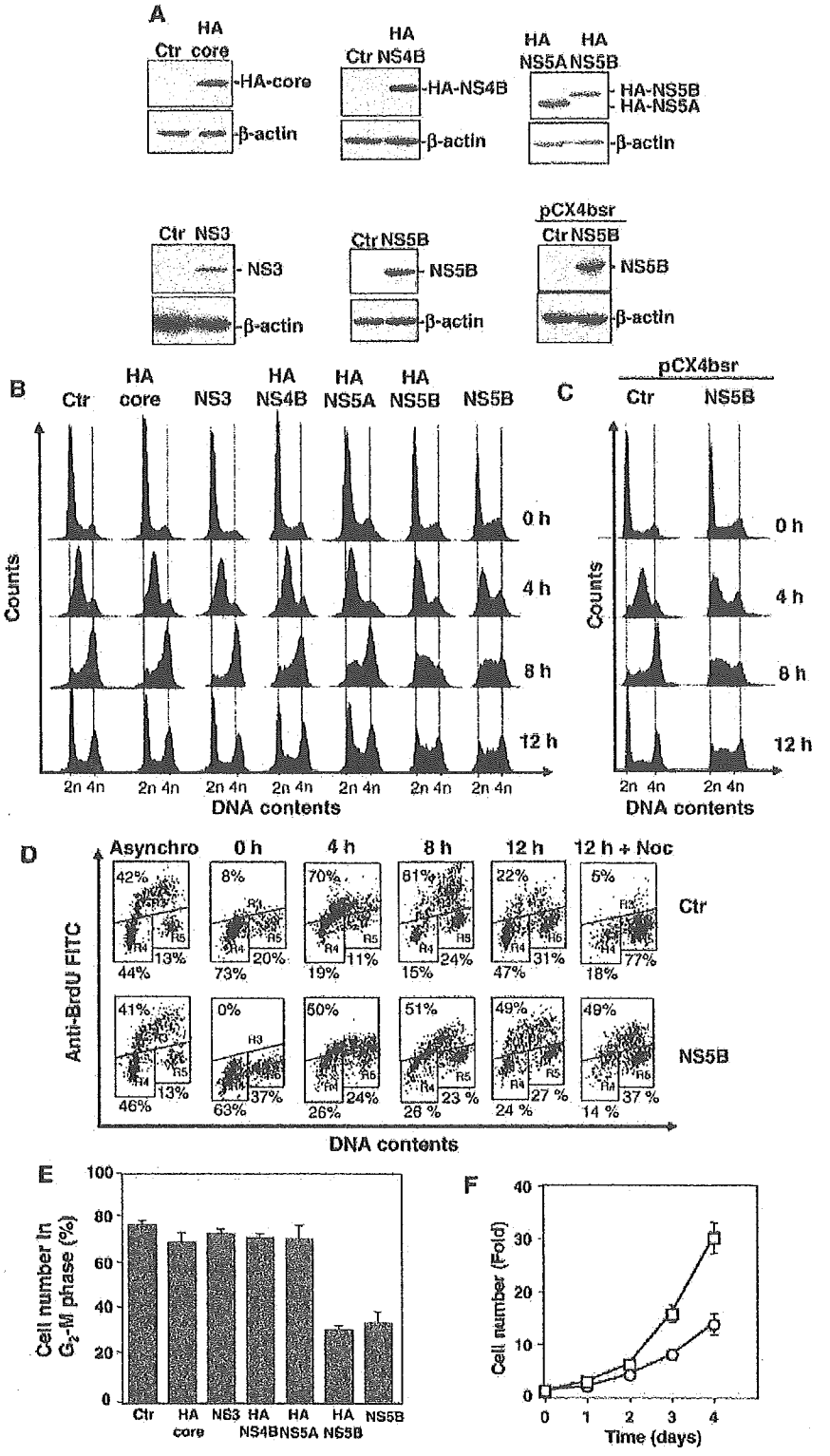

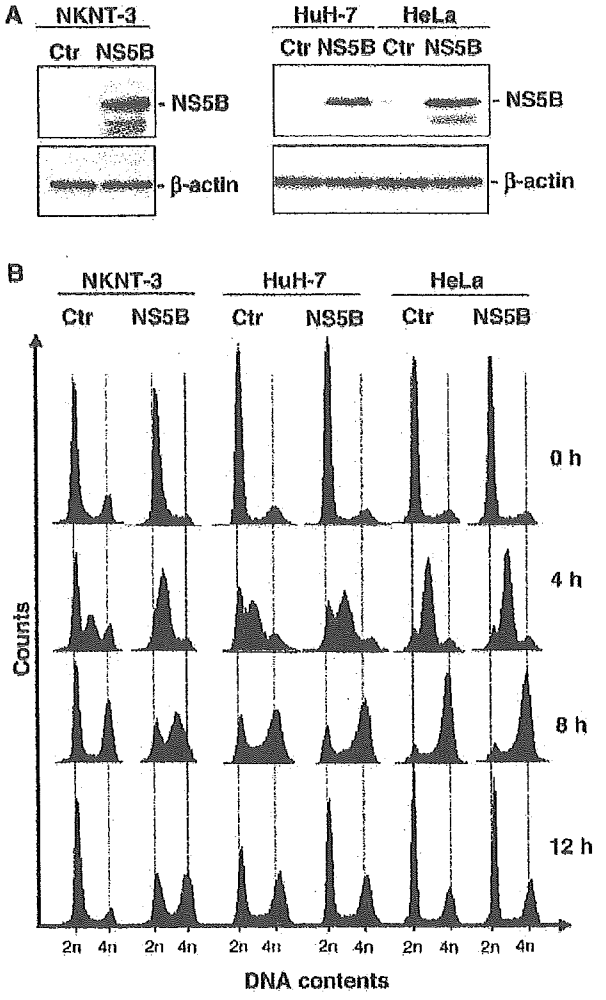

Fig. 2. NS5B delays S phase progression in another immortalized human hepatocytes. (A) Western blot analysis of NKNT-3, HuH-7, and HeLa cells infected with pCXbsr retrovirus encoding NS5B. The pCXbsr retrovirus was used as a control infection (Ctr). Anti-NS5B and anti-β-actin antibodies were used for the immunoblotting analysis. (B) Cell cycle analysis of NKNT-3, HuH-7, and HeLa cells expressing NS5B. NKNT-3, HuH-7, and HeLa cells that expressed NS5B (NS5B series) were synchronized, and cell cycle progression was analyzed as indicated in Fig. 1B. NKNT-3, HuH-7, and HeLa cells that were infected with the pCXbsr retrovirus were also analyzed as a control (Ctr series).

induced by NS5B. To evaluate this hypothesis, we examined whether or not PH/NS5B and NKNT-3 cells expressing NS5B (NK/NS5B) induce the expression of IFN-β. RT-PCR analysis clearly indicated that they did, and, at the same time, we found that HuH-7 and HeLa cells did not, despite their expression of NS5B (Fig. 3A). We next examined whether or not S phase progression is delayed in PH5CH8 and NKNT-3 cells treated with IFN-β prior to release from the G1/S boundary. As we expected, the S phase progression was stalled in PH5CH8 and NKNT-3 cells treated with IFN-β (Fig. 3B). We also observed that IFN-γ did not possess this activity of IFN-β (data not shown). These results suggest that the induction of IFN-β is implicated in the cell cycle delay in two immortalized human hepatocyte cell lines, PH5CH8 and NKNT-3.

To confirm the effect of IFN-β on cell cycle delay, we further examined whether or not treatment with anti-IFN-β neutralizing antibody can restore the cell cycle delay in PH/NS5B cells. The results showed that this treatment canceled the delay of S phase progression in PH/NS5B cells (Fig. 4A). BrdUrd incorporation analysis also showed that the proportion of cells reaching the G2-M phase was increased by the treatment with anti-IFN-β antibody in PH/NS5B cells (Fig 4B). These observations indicated that the expression of IFN-β mediated cell cycle delay during the S phase in PH/NS5B cells and suggested that the expression of NS5B induced IFN-β in PH5CH8 and NKNT-3 cells even without replication of the viral genome.

Activation of TLR3 signaling pathway by NS5B

Since IFN-β is known as a major cytokine induced by the activation of the TLR3 and TLR4 signaling pathways (Takeda et al., 2003), we next focused on which TLR pathway was activated for the production of IFN-β in PH/NS5B cells. To answer this question, TLR3- and TLR4-specific siRNAs were used to knock down TLR3 and TLR4 expression in PH/NS5B cells. TLR3 and TLR4 mRNAs were drastically decreased in PH/NS5B cells transfected with TLR3 and TLR4 siRNAs, respectively, but not in PH/NS5B cells transfected with GL2 siRNA (Elbashir et al., 2001) used as a control (Fig. 5A). This result indicates that the siRNAs used specifically contribute well to the degradation of TLR3 and TLR4 mRNAs. In this condition, IFN-β mRNA was significantly decreased in only PH/NS5B cells transfected with TLR3 siRNA (Fig. 5A), indicating that IFN-β expression in PH/NS5B cells is mediated through the TLR3 signaling pathway. The growth rate of PH/NS5B cells transfected with TLR3 siRNA was also accelerated, although TLR4 siRNA showed a rather lethal effect (Fig. 5B).

Fig. 1. HCV NS5B causes the delay of S phase progression. (A) Expression of HCV proteins in human cells introduced by retrovirus-mediated gene transfer. Western blot analysis of PH5CH8 cells infected with pCXbsr retroviruses encoding HCV proteins (HA-core, NS3, HA-NS4B, HA-NS5A, HA-NS5B, and NS5B) or pCX4bsr retrovirus encoding NS5B. pCXbsr or pCX4bsr retrovirus was used as a control infection (Ctr). Anti-HA (3F10, Roche), anti-NS3 (Novacastra), anti-NS5B, and anti-β-actin (Sigma) antibodies were used for the immunoblotting analysis. (B) Cell cycle analysis of PH5CH8 cells expressing HCV proteins. PH5CH8 cells that expressed HA-core, NS3, HA-NS4B, HA-NS5A, HA-NS5B, or NS5B were synchronized at G1/S boundary, and then cell cycle progression was monitored by flow cytometry after the release of the cells into the S phase at the indicated times. PH/Ctr cells that were infected with pCXbsr retrovirus were also analyzed as a control. (C) Cell cycle analysis of PH5CH8 cells infected with pCX4bsr retrovirus encoding NS5B. The cell cycle analysis was performed as described in panel B. (D) BrdUrd incorporation analysis of PH/Ctr and PH/NS5B cells. Cell cycle distribution of dot-plots of BrdUrd fluorescence versus DNA contents was analyzed in asynchronous or synchronized PH/Ctr and PH/NS5B cells. To measure the cells reaching the G2-M phase at 12 h after release, the cells were accumulated by Noc treatment. (E) Analysis of the cells reaching the G2-M phase. The percentage of cells at that phase was assessed by Noc treatment as indicated in panel D. The data are means ± SD of values from three independent experiments. (F) Growth curve of PH/Ctr and PH/NS5B cells. PH/Ctr (squares) or PH/NS5B (circles) were plated onto 6-well plates (3×10^4 cells per well), and the kinetics of cell proliferation during 4 days in culture were determined by trypan blue treatment. The data indicate average values ± SD from three independent experiments.

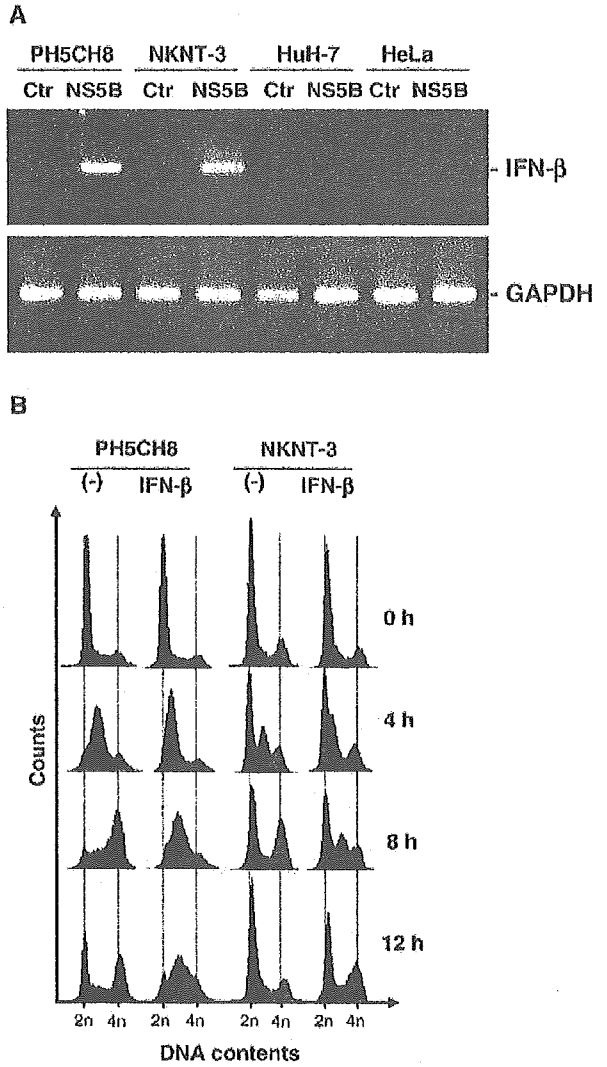

Fig. 3. IFN-β mediates the delay of S phase progression by NS5B. (A) RT-PCR analysis of IFN-β mRNA. The total RNAs were extracted from PH5CH8, NKNT-3, HuH-7, and HeLa cells (Ctr and NS5B series) and were subjected to RT-PCR analysis using primer sets for IFN-β (341 bp) and GAPDH (587 bp). (B) Cell cycle analysis of PH5CH8 and NKNT-3 cells treated with or without IFN-β. PH5CH8 and NKNT-3 cells were treated with or without IFN-β (500 IU/ml) at 12 h prior to release, and cell cycle progression was analyzed as indicated in Fig. 1B.

Furthermore, BrdUrd incorporation analysis using the Noc treatment revealed that 56% of PH/NS5B cells transfected with TLR3 siRNA reached the G2-M phase at 12 h after release, while only 33% of PH/NS5B cells transfected with GL2 siRNA reached that phase (Fig. 5C). The percentage of G2-M phase cells at 12 h after release was also 34% in PH/NS5B cells transfected with TLR4 siRNA, although the growth rate of these cells was lower than that of cells transfected with GL2 siRNA. These results indicated that the induction of IFN-β by NS5B expression was mediated through the activation of the TLR3 signaling pathway. This, in turn, demonstrated that TLR3 siRNA could override the delay of S phase progression in PH/NS5B cells.

To obtain further evidence that the induction of IFN-β by NS5B is mediated through TLR3, we prepared human embryonic kidney (HEK) 293 cells stably expressing TLR3 derived from PH5CH8 cells since it has been reported that ectopic expression of TLR3 can reconstruct the TLR3 signaling pathway in HEK293 cells (Alexopoulou et al., 2001). First, HEK293 cells were infected with retrovirus pCXbsr encoding NS5B or pCXbsr as a negative control (Ctr), yielding HEK293 cells (HEK/NS5B) stably expressing NS5B and control HEK293 cells (HEK/Ctr). Next, HEK/NS5B and HEK/Ctr cells were infected with

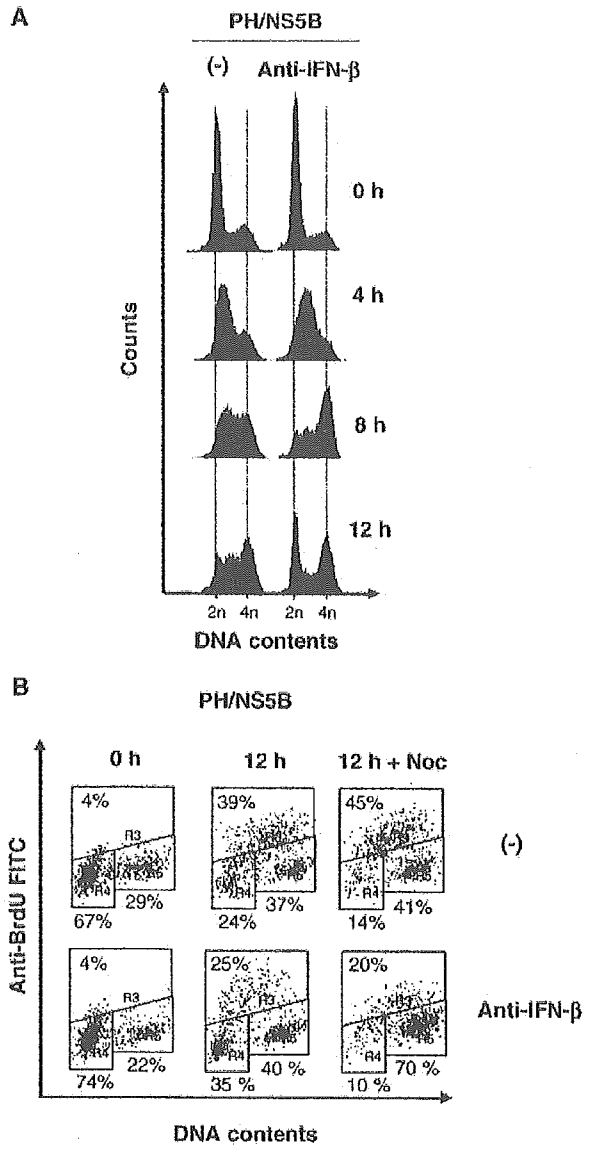

Fig. 4. Treatment with anti-IFN-β antibody canceled the delay of S phase progression. (A) Cell cycle analysis of PH/NS5B cells treated with or without anti-IFN-β antibody. PH/NS5B cells were treated with anti-IFN-β antibody (70 U/ml, Oxford Biotechnology) during cell cycle synchronization and after release from the G1/S boundary. (B) BrdUrd incorporation analysis of PH/NS5B cells treated with or without anti-IFN-β antibody. The antibody was used as indicated in panel A. Noc was used as indicated in Fig. 1D.

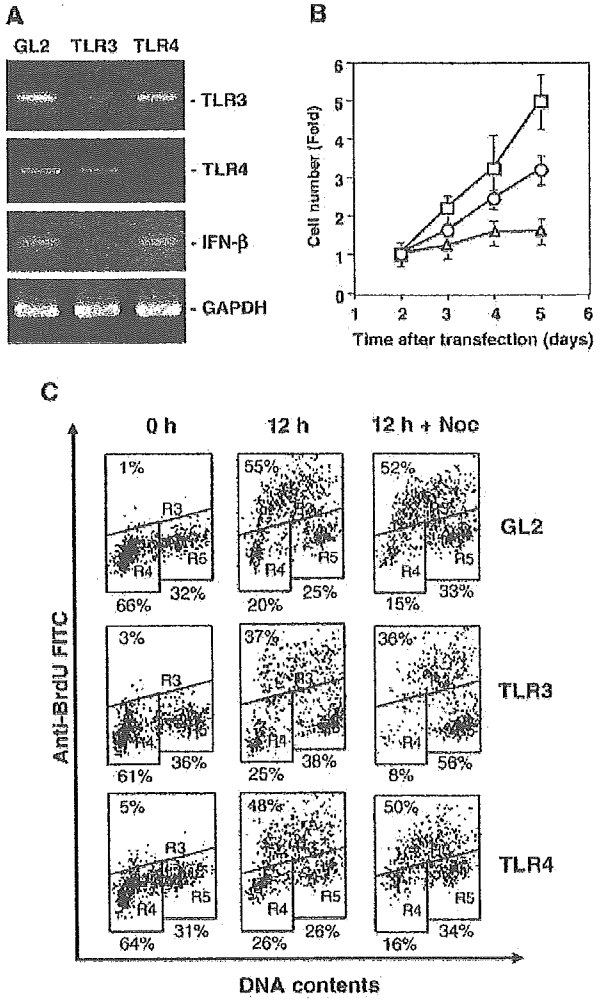

Fig. 5. Activation of IFN-β gene by NS5B is mediated through the TLR3 signaling pathway. (A) Down-regulation of IFN-β mRNA by transfection of TLR3 siRNA. PH/NS5B cells were transfected with dsRNA duplexes targeting TLR3, TLR4, or luciferase GL2. After 3 days, the expression levels of TLR3, TLR4, IFN-β, and GAPDH mRNAs were examined by RT-PCR. (B) Growth curve of PH/NS5B cells transfected with siRNAs. After 2 days of transfection, the proliferation kinetics of PH/NS5B cells transfected with GL2 (circles), TLR3 (squares), and TLR4 (triangles) siRNAs were analyzed as indicated in Fig. 1F. (C) BrdUrd incorporation analysis of PH/NS5B cells transfected with GL2, TLR3, and TLR4 siRNAs. After 2 days of transfection, the cells were synchronized, and cell cycle progression was analyzed as indicated in Fig. 1D.

retrovirus pCXpur encoding TLR3 or pCXpur as a negative control, yielding cells stably expressing TLR3 and control HEK293 cells. The expression of NS5B or TLR3 was confirmed by Western blot analysis (Fig. 6A). We then performed a dual-luciferase reporter assay using an IFN-β gene promoter. The results revealed that the luciferase activity was enhanced in only the HEK293 cells stably expressing both NS5B and TLR3 (Fig. 6B). This suggests that TLR3 mediates NS5B's induction of IFN-β. However, since the enhancement of luciferase activity was approximately two-fold, we failed to detect the enhancement of the mRNA expression levels for IFN-β and one of its target genes, ISG56 (data not shown). To accurately assess the enhancement, high expression levels of NS5B and TLR3 in HEK293 cells will be needed.

The RIG-I-mediated signaling pathway is not implicated in the induction of IFN-β in PH/NS5B cells

Recently, RIG-I, a cellular DExD/H box helicase, was found to be a double-stranded RNA (dsRNA) binding protein that functions independently of TLR3 to induce IFN-β in response to viral infection (Yoneyama et al., 2004). Since another recent study showed that both the TLR3- and RIG-I-mediated signaling pathways are functional in PH5CH8 cells (Li et al., 2005a, 2005b), we examined whether or not the RIG-I-mediated signaling pathway is involved in NS5B's induction of IFN-β. First, PH/NS5B and PH/Ctr cells were infected with retrovirus pCXpur encoding myc-tagged RIG-IC, a dominant negative inhibitor of RIG-I harboring only the helicase domain but not the two N-terminal CARD domains (Yoneyama et al., 2004), or pCXpur as a negative control. Cells that stably expressed myc-tagged RIG-IC were thus obtained. The expression of myc-

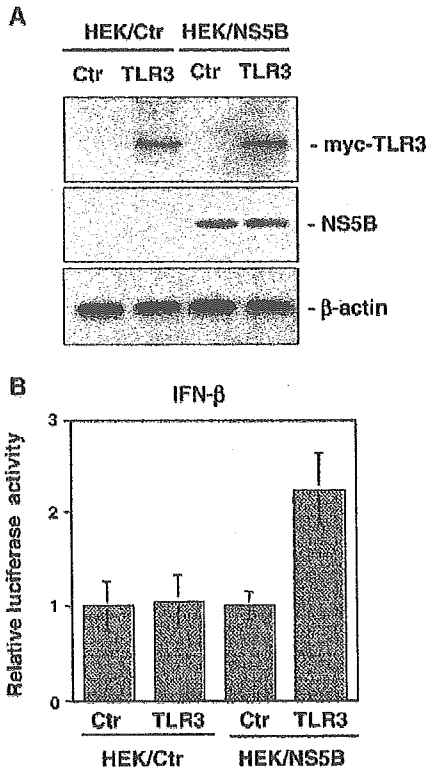

Fig. 6. Ectopic expression of TLR3 enhances the IFN-β gene promoter in only the HEK293 cells stably expressing NS5B. (A) Expression of TLR3 and NS5B in HEK293 cells introduced by retrovirus-mediated gene transfer. Western blot analysis of HEK/Ctr or HEK/NS5B cells infected with pCXpur retrovirus encoding myc-tagged TLR3 was performed. The pCXpur retrovirus was used as a control infection. Anti-myc, anti-NS5B, and anti-β-actin antibodies were used for the immunoblotting analysis. (B) Dual luciferase reporter assay of the IFN-β gene promoter. The cells shown in panel A were transfected with pIFN-β(-125)-Luc, and the dual luciferase assay was performed as described previously (Dansako et al., 2003). Data are means ± SD from three independent triplicate experiments.

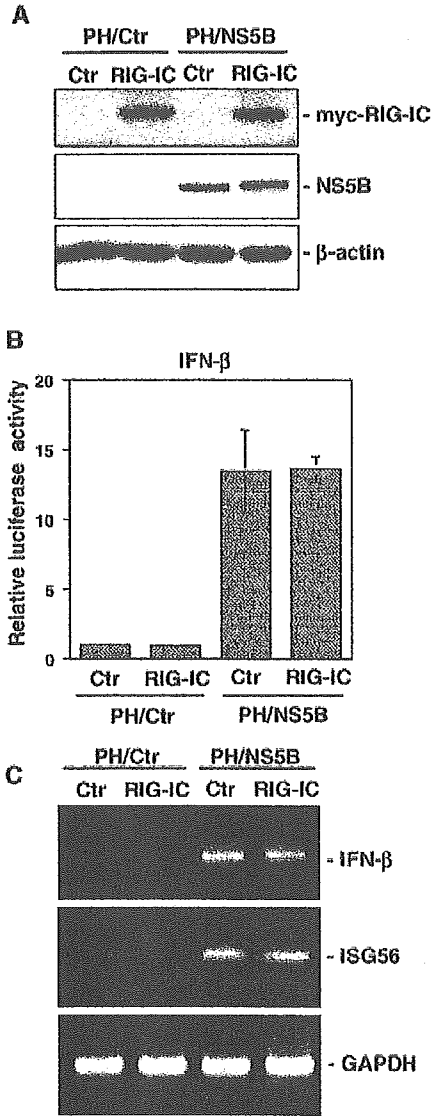

Fig. 7. Induction of IFN-β by NS5B is not mediated through the RIG-I signaling pathway. (A) Expression of RIG-IC and NS5B in PH5CH8 cells introduced by retrovirus-mediated gene transfer. Western blot analysis of PH/Ctr or PH/NS5B cells infected with pCXpur retrovirus encoding myc-tagged RIG-IC was performed. The pCXpur retrovirus was used as a control infection. Anti-myc, anti-NS5B, and anti-β-actin antibodies were used for the immunoblotting analysis. (B) Dual luciferase reporter assay of the IFN-β gene promoter. The cells shown in panel A were transfected with pIFN-β(-125)-Luc, and the dual luciferase assay was performed as indicated in Fig. 6B. (C) RT-PCR analysis of IFN-β and ISG56 mRNAs. The total RNAs were extracted from the cells shown in panel A and subjected to RT-PCR analysis using primer sets for IFN-β (341 bp), ISG56 (320 bp), and GAPDH (587 bp).

tagged RIG-IC was confirmed by Western blot analysis (Fig. 7A). Using PH/Ctr cells stably expressing myc-tagged RIG-IC, we confirmed that IFN-β production was markedly suppressed after infection with Sendai virus (data not shown), as initially observed in Newcastle disease virus infection (Yoneyama et al., 2004). This indicates that RIG-IC functions as a dominant negative inhibitor of RIG-I in PH5CH8 cells. We then performed a dual-luciferase reporter assay using an *IFN-β* gene promoter. The results revealed that the enhancement of luciferase activity in PH/NS5B cells was not suppressed regardless of RIG-IC expression (Fig. 7B). Furthermore, the mRNA expression levels for IFN-β and one of its target genes, ISG56, were also unchanged by the expression of RIG-IC (Fig. 7C). These results suggest that NS5B's induction of IFN-β is not mediated through the RIG-I signaling pathway.

NS5B does not interact with TLR3 adaptor protein

Since we showed that NS5B's induction of IFN-β was mediated through the TLR3 but not the RIG-I signaling pathway, we further examined the mechanism underlying IFN-β induction by testing the possibility of interaction between NS5B and the TLR3 adaptor protein TRIF (Yamamoto et al., 2002). We prepared HEK/NS5B cells stably expressing myc-tagged NS5A or myc-tagged TRIF and examined whether or not NS5B interacts with TRIF by an immunoprecipitation method following Western blot analysis. The results clearly showed that NS5B and myc-tagged NS5A were co-immunoprecipitated by anti-myc antibody as reported previously (Shirota et al., 2002). However, co-immunoprecipitation of NS5B and myc-tagged TRIF was clearly not observed (Fig. 8). This result suggests that the activation of the TLR3 signaling pathway by NS5B occurs through one or more factors other than TRIF.

Induction of IFN-β depends on RNA-dependent RNA polymerase (RdRp) activity of NS5B

Since dsRNA, an intermediate of viral replication, is known as a natural ligand for the activation of TLR3 (Alexopoulou et

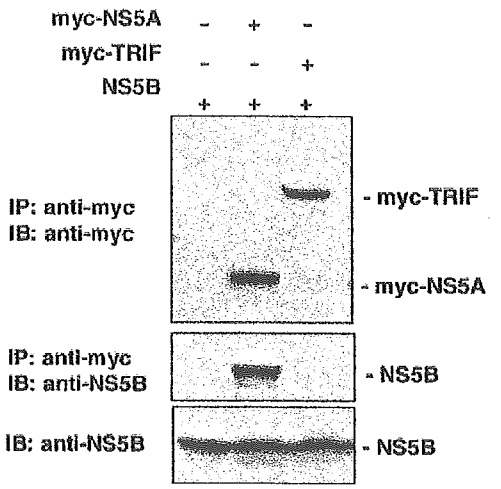

Fig. 8. NS5B does not interact with TRIF. HEK/NS5B cells were infected with pCXpur retrovirus encoding myc-tagged NS5A (middle lane) or myc-tagged TRIF (right lane). pCXpur retrovirus was used as a control infection (left lane). Cell lysate was immunoprecipitated (IP) with anti-myc antibody-conjugated agarose beads. The immunoprecipitates were resolved by SDS-PAGE, and anti-myc (upper panel) and anti-NS5B (middle panel) antibodies were used for the immunoblotting (IB) analysis. To confirm the expression level of NS5B, cell lysates were subjected to immunoblotting analysis using anti-NS5B antibody (lower panel).

al., 2001; Takeda et al., 2003), we next examined whether or not the induction of IFN-β in human hepatocytes expressing NS5B (591 amino acids; amino acids 2420 to 3010 in the HCV-1b genotype) (Kato et al., 1990) depends on NS5B's RdRp activity. Since this activity is already well characterized (Hagedorn et al., 2000), we constructed several NS5B mutants to evaluate this subject (Fig. 9A). One is the substitution mutant G2736V of the GDD motif (amino acids 2736–8) located in the catalytic site, and the other is the deletion mutant Δ2575–7 (R2753T, K2754S, and Δ2575–7) at the priming and interrogation sites, all of which are essential for NS5B's RdRp activity (Behrens et al., 1996; Bressanelli et al., 2002). We also constructed three carboxyl-truncated forms (ΔC21, ΔC56, and ΔC97, lacking 21, 56, and 97 amino acids, respectively) of NS5B. These truncated mutants of NS5B lack the last 21 hydrophobic amino acids, which are necessary and sufficient to target NS5B to the cytosolic side of the endoplasmic reticulum (ER) membrane (Schmidt-Mende et al., 2001; Yamashita et al., 1998). Although ΔC21 and ΔC56, but not ΔC97, possess RdRp activity in vitro, ΔC56 shows higher RdRp activity than ΔC21 because only the latter possesses a regulatory motif inhibiting RNA binding and polymerase activity (Leveque et al., 2003). We prepared PH5CH8 cells stably expressing these NS5B mutants and then performed cell cycle analysis using these

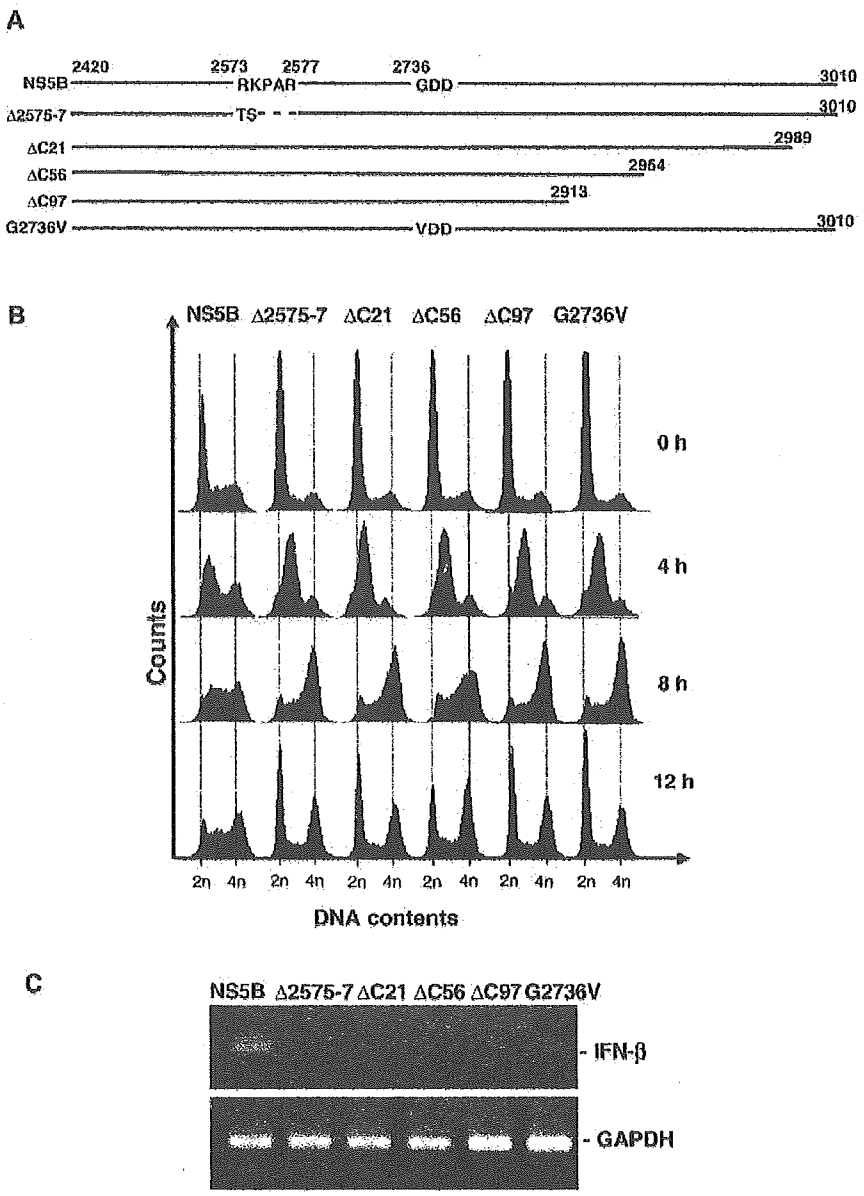

Fig. 9. The RdRp activity of NS5B anchoring on ER membrane is required for induction of IFN-β and following the delay of S phase progression. (A) Schematic presentation of the NS5B mutants used. Only amino acid sequences in the mutated regions of NS5B are indicated. (B) Cell cycle analysis of PH/NS5B and PH5CH8 cells expressing NS5B mutants. Cell cycle distribution was analyzed as described in Fig. 1B. (C) RT-PCR analysis of IFN-β mRNA in PH/NS5B and PH5CH8 cells expressing NS5B mutants. RT-PCR analysis was performed as described in Fig. 3A.

prepared cells. The results revealed no effect on S phase progression in the PH5CH8 cells expressing NS5B mutants (Fig. 9B), although PH5CH8 cells expressing ΔC56 showed a slight delay of S phase progression. Induction of IFN-β mRNA was also not observed in the PH5CH8 cells expressing NS5B mutants (Fig. 9C). These results revealed that the delay of S phase progression and the induction of IFN-β depend on the RdRp activity of NS5B, and these effects are coupled with ER membrane anchorage of NS5B in cells.

To examine the activation of IRF3, a factor specifically induced by stimulated TLR3 or TLR4, by the expression of NS5B and its mutants, we performed a dual-luciferase reporter assay using a synthetic promoter having five repeats of the consensus ISRE, which was the same as the IRF3 target sequence in the *IFN-β* gene promoter (Fig. 10A) and an intrinsic *IFN-β* gene promoter (Fig. 10B). The results showed that the luciferase activity was enhanced approximately five-fold (Fig. 10A) and eight-fold (Fig. 10B) only in PH/NS5B cells,

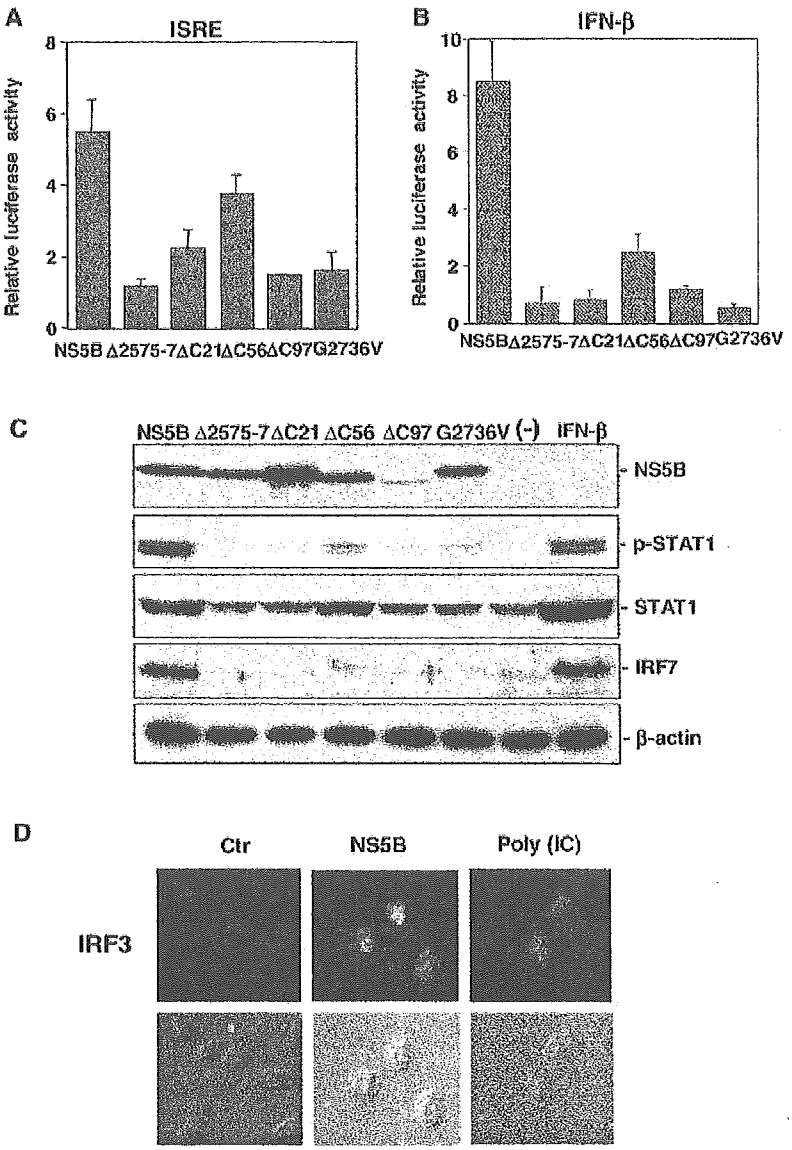

Fig. 10. NS5B full form is required for activation of IRF3 target sequences and IFN-β signaling pathway. (A) Dual luciferase reporter assay toward IRF3 target sequences. PH5CH8 cells were transfected with the pISRE-Luc (Stratagene) and pCXbsr encoding NS5B or its mutant, and the dual luciferase assay was performed as indicated in Fig. 6B. The lysates of cells transfected with pCXbsr were used as a control. (B) Dual luciferase reporter assay of the IFN-β gene promoter. Dual luciferase assay was performed as described in panel A except using pIFN-β(-125)-Luc instead of pISRE-Luc. (C) Western blot analysis of the components involved in the IFN-β signaling pathway. The lysates of PH/NS5B and PH5CH8 cells expressing NS5B mutants were subjected to immunoblotting using anti-NS5B, anti-p-STAT1(Y701), anti-STAT1, anti-IRF7, and anti-β-actin antibodies. PH5CH8 cells treated with or without IFN-β (500 IU/ml for 24 h) were also analyzed as a control. (D) Subcellular distribution of endogenous IRF3. PH/Ctr and PH/NS5B cells were processed and stained with anti-IRF3 antibody and an FITC-conjugated secondary antibody. PH5CH8 cells treated with poly (IC) were also used as a positive control.

suggesting that IRF3 is activated by the NS5B full form. Interestingly, however, luciferase activity was enhanced approximately four-fold (Fig. 10A) and three-fold (Fig. 10B) in PH5CH8 cells expressing ΔC56, although the enhancement was not as great as the five-fold (Fig. 10A) and eight-fold (Fig. 10B) in PH/NS5B cells, respectively. We then examined the phosphorylation status of STAT1 on Y701 and the level of IRF7, one of the downstream targets of the IFN-β signaling pathway (Katze et al., 2002). Western blot analysis revealed marked phosphorylation of STAT1 and IRF7 expression in PH/NS5B cells as well as in PH5CH8 cells treated with IFN-β (Fig. 10C). Although slight phosphorylation of STAT1 was observed in the PH5CH8 cells expressing ΔC56, IRF7 expression was not observed (Fig. 10C). Unlike PH/NS5B cells and PH5CH8 cells expressing ΔC56, neither the phosphorylation of STAT1 nor the expression of IRF7 was detected in PH5CH8 cells expressing other NS5B mutants. These results indicated that ΔC56 had an extremely low ability to induce IFN-β after activation of TLR3, although ΔC56 was still able to enhance the IRF3 target promoter. To obtain further evidence of the activation of IRF3, we examined the subcellular distribution of endogenous IRF3 in PH/Ctr and PH/NS5B

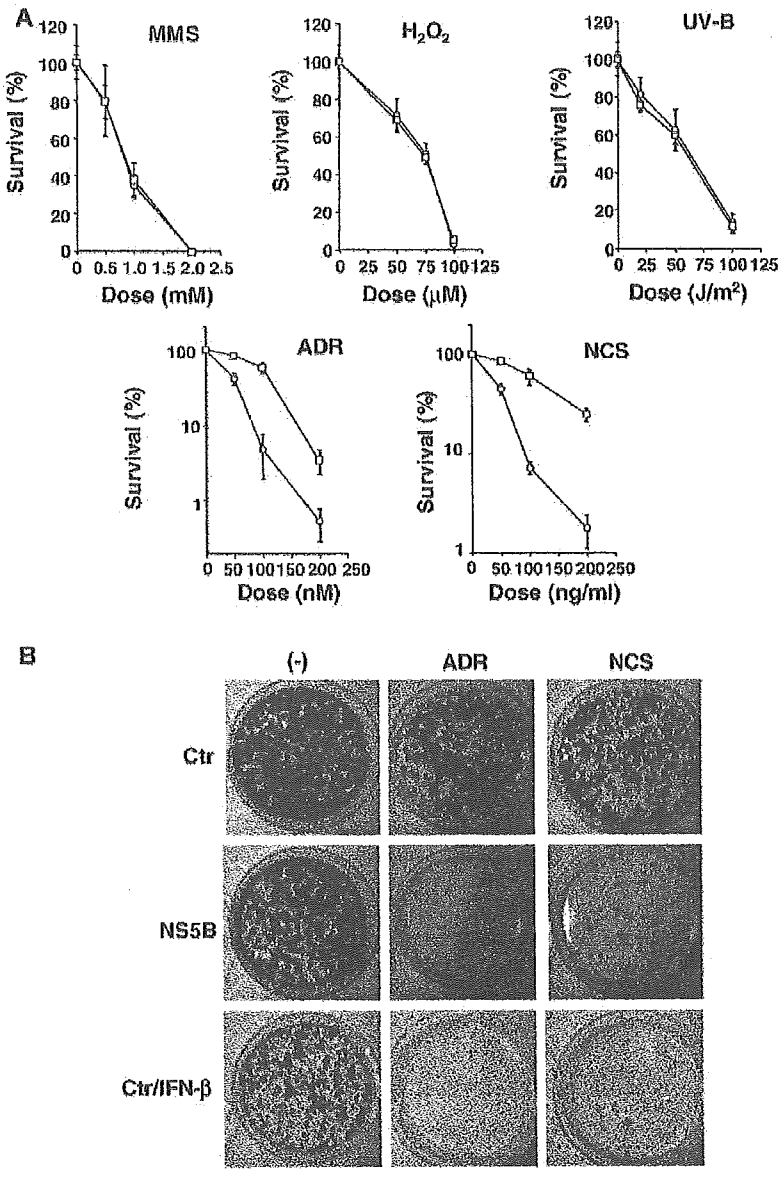

Fig. 11. Sensitivity of PH/NS5B cells against DNA-damaging reagents. (A) Clonogenic assays for PH/Ctr (square) and PH/NS5B (circle) cells after treatment with increasing doses of DNA-damaging reagents. Cells were treated with MMS, H_2O_2, UV-B, ADR, and NCS. Ten days after the treatment, cells were fixed and stained with Coomassie brilliant blue. Only colonies containing >50 cells were scored as being derived from viable clonogenic cells. Data are means ± SD from two independent triplicate experiments. (B) PH/Ctr, PH/NS5B, and IFN-β-treated (20 IU/ml) PH/Ctr cells were treated with ADR (100 nM) or NCS (100 ng/ml). The panels show survived colonies that are stained with Coomassie brilliant blue at 10 days after the treatment.